◀ **Fig. 2** Changes from baseline in the regional wall thickness of the LV at 3 months and 1 year follow-up. **a–d** Images of the end-diastolic (**a**, **c**) and end-systolic (**b**, **d**) phase at baseline (**a**, **b**) and at the 3-month follow-up (**c**, **d**). The calculated wall thickness of each segment is shown in **e** (end-diastolic phase) and **f** (end-systolic phase), and the percent wall thickening is shown in **g**. The surgical specimens were obtained from the LV apical core removed at the time of LVAS implantation (**h**), and the needle biopsy of the LV anterior wall at the time of LVAS removal (**i**). Specimens were stained with hematoxylin–eosin (HE) by a conventional technique. **j** After LVAS implantation, the BNP level declined and reached a plateau. After myoblast sheet implantation, the BNP levels declined again to within the normal range

the anterior to lateral surface of the dilated heart through a left lateral thoracotomy.

Off-pump tests performed 8 weeks and 3 months after transplantation revealed that the ejection fraction was improved from 26 to 46%, and the LVDd from 49 to 53 mm (Fig. 1b, c). These data met the criteria for the explantation of LVAS, which was subsequently performed. Comparison of the wall motion pre- and post-treatment by color kinesis revealed improvement first on the anterior and lateral surfaces and then, in the longer term, on the other surface (Fig. 2). After starting the LVAS, the patient's brain natriuretic peptide (BNP) levels had gradually declined and reached a plateau. Subsequently, after myoblast sheet implantation, the BNP levels declined again and reached the normal range (Fig. 2j). The patient was discharged 7 months after myoblast sheet transplantation and has been an out-patient for more than 1 year. Regarding his clinical course after both cell sheet transplantation and LVAD removal, a Holter cardiogram demonstrated that no life-threatening arrhythmia had occurred.

Discussion

Menasche et al. [3] recently concluded that myoblast injections combined with coronary surgery in patients with depressed LV function fail to improve echocardiographic heart function. The proportion of injected cells surviving to engraft the infarcted myocardium is very low, owing to injected cells leaking from the intended region and being carried to other organs [4]. This loss of cells has therefore limited the applicability of this form of myoblast cell therapy [3].

To overcome these problems, we have developed a novel cell delivery system [5] that uses myoblast cell sheets, and performed animal investigations to guide clinical trials [4]. Using temperature-responsive tissue engineering techniques, we were able to transplant a larger numbers of cells, with greater viability, than by myoblast injection, and such cell sheets engrafted to the failed myocardium in rats led to improvements in cardiac function and tissue remodeling [4]. Although the myoblasts cannot transdifferentiate to cardiomyocytes, the myoblast sheets produce cytokines such as hepatocyte growth factor (HGF), which may have a positive impact on c-Met-expressing damaged myocardium [4], thus leading to the attenuation of fibrosis, angiogenesis, and recruitment of stem cells induced by paracrine cytokines.

In cellular therapy for cardiac disease, arrhythmogenesis is expected to occur in animal models and in clinical trials [3]; however, life-threatening arrhythmias have not been clinically observed after autologous cell sheet transplantation. In the case of injection, scarring of the myocardium is likely, and such scars can induce arrhythmias. Using our cell delivery technique, there may be less risk for inducing arrhythmia. Myoblasts have a weak electrical potential, and it may thus be possible for them to induce arrhythmia if they survive in the myocardium. However, cell sheets may not induce arrhythmia owing to their attachment to the epicardium.

In conclusion, autologous myoblast cell sheet transplantation may positively contribute to the improvement of the clinical condition of patients with DCM, allow the discontinuation of LVAS, and avoid heart transplantation. This therapy therefore shows promise for clinical myocardial regeneration in patients with end-stage DCM.

References

1. Dandel M, Weng Y, Siniawski H, Potapov E, Lehmkuhl HB, Hetzer R. Long-term results in patients with idiopathic dilated cardiomyopathy after weaning from left ventricular assist devices. Circulation. 2005;112:I37–45.
2. Hata H, Matsumiya G, Miyagawa S, et al. Grafted skeletal myoblast sheets attenuate myocardial remodeling in pacing-induced canine heart failure model. J Thorac Cardiovasc Surg. 2006;132:918–24.
3. Menasche P, Alfieri O, Janssens S, et al. The myoblast autologous grafting in ischemic cardiomyopathy (MAGIC) trial: first randomized placebo-controlled study of myoblast transplantation. Circulation. 2008;117:1189–200.
4. Memon IA, Sawa Y, Fukushima N, et al. Repair of impaired myocardium by means of implantation of engineered autologous myoblast sheets. J Thorac Cardiovasc Surg. 2005;130:1333–41.
5. Miyagawa S, Sawa Y, Sakakida S, et al. Tissue cardiomyoplasty using bioengineered contractile cardiomyocyte sheets to repair damaged myocardium: their integration with recipient myocardium. Transplantation. 2005;80:1586–95.

Myoblast Sheet Can Prevent the Impairment of Cardiac Diastolic Function and Late Remodeling After Left Ventricular Restoration in Ischemic Cardiomyopathy

Shunsuke Saito,[1] Shigeru Miyagawa,[1] Taichi Sakaguchi,[1] Yukiko Imanishi,[1] Hiroko Iseoka,[1] Hiroyuki Nishi,[1] Yasushi Yoshikawa,[1] Satsuki Fukushima,[1] Atsuhiro Saito,[1] Tatsuya Shimizu,[2] Teruo Okano,[2] and Yoshiki Sawa[1,3]

Background. Impairment of diastolic function and late remodeling are concerns after left ventricular restoration (LVR) for ischemic cardiomyopathy. This study aims to evaluate the effects of combined surgery of myoblast sheets (MS) implantation and LVR.

Methods. Rat myocardial infarction model was established 2 weeks after left anterior descending artery ligation. They were divided into three groups: sham operation (n=15; group sham), LVR by plicating the infracted area (n=15; group LVR), and MS implantation with LVR (n=15; group LVR+MS).

Results. Serial echocardiographic study revealed significant LV redilatation and decrease of ejection fraction 4 weeks after LVR in group LVR. MS implantation combined with LVR prevented those later deteriorations of LV function in group LVR+MS. Four weeks after the operation, a hemodynamic assessment using a pressure-volume loop showed significantly preserved diastolic function in group LVR+MS; end-diastolic pressure (LVR vs. LVR+MS: 9.0±6.6 mm Hg vs. 2.0±1.0 mm Hg, $P<0.05$), end-diastolic pressure-volume relationship (LVR vs. LVR+MS 42±23 vs. 13±6, $P<0.05$). Histological examination revealed cellular hypertrophy and LV fibrosis were significantly less and vascular density was significantly higher in group LVR+MS than in the other two groups. Reverse transcription polymerase chain reaction demonstrated significantly suppressed expression of transforming growth factor-beta, Smad2, and reversion-inducing cysteine-rich protein with Kazal motifs in group LVR+MS.

Conclusions. MS implantation decreased cardiac fibrosis by suppressing the profibrotic gene expression and attenuated the impairment of diastolic function and the late remodeling after LVR. It is suggesting that MS implantation may improve long-term outcome of LVR for ischemic heart disease.

Keywords: Ischemic cardiomyopathy, Left ventricular restoration, Regenerative therapy, Myoblast sheet, Diastolic function.

(*Transplantation* 2012;93: 1108–1115)

Ischemic heart disease is one of the leading causes of death and disability in most of the industrialized countries and recognized as a major public health issue. Progression to end-stage heart failure involves massive loss of cardiomyocyte, massive fibrosis, and progressive remodeling of the ventricles. Left ventricular (LV) volume reduction surgery or LV restoration (LVR) surgery has been introduced as a surgical treatment of patients with dilated LV and chronic heart failure (*1*, *2*), and has been shown to reduce the LV volume, increase the ejection fraction, and improve ventricular function (*3*, *4*).

The authors declare no funding or conflicts of interest.

[1] Department of Cardiovascular Surgery, Osaka University Graduate School of Medicine, Suita, Osaka, Japan.

[2] Institute of Advanced Biomedical Engineering and Science, Tokyo Women's Medical University, Tokyo, Japan.

[3] Address correspondence to: Yoshiki Sawa, M.D., Department of Cardiovascular Surgery, Osaka University Graduate School of Medicine (E1), 2-2 Yamada-Oka, Suita, Osaka 565-0871, Japan.

E-mail: sawa@surg1.med.osaka-u.ac.jp

S.S. participated in research design, the performance of the research, data analysis, and the writing of the manuscript; T.S. participated in research design and data analysis; S.M. participated in research design and data analysis, and the writing of the manuscript; Y.I. performed quantitative analysis of engrafted myoblasts survival; H.I. performed histological analysis of engrafted myoblasts survival; H.N. participated in the performance of the research; Y.Y. participated in the performance of the research; S.F. participated in the performance of the research; A.S. participated in research design and data analysis; T.S. contributed to the development of the temperature-responsive culture dish and cell sheet implantation technique; T.O. contributed to the development of the temperature-responsive culture dish and cell sheet implantation technique; and Y.S. participated in research design, data analysis, and the writing of the manuscript.

Received 28 June 2011. Revision requested 20 July 2011.

Accepted 10 February 2012.

ISSN: 0041-1337/12/9311-1108

DOI: 10.1097/TP.0b013e31824fd803

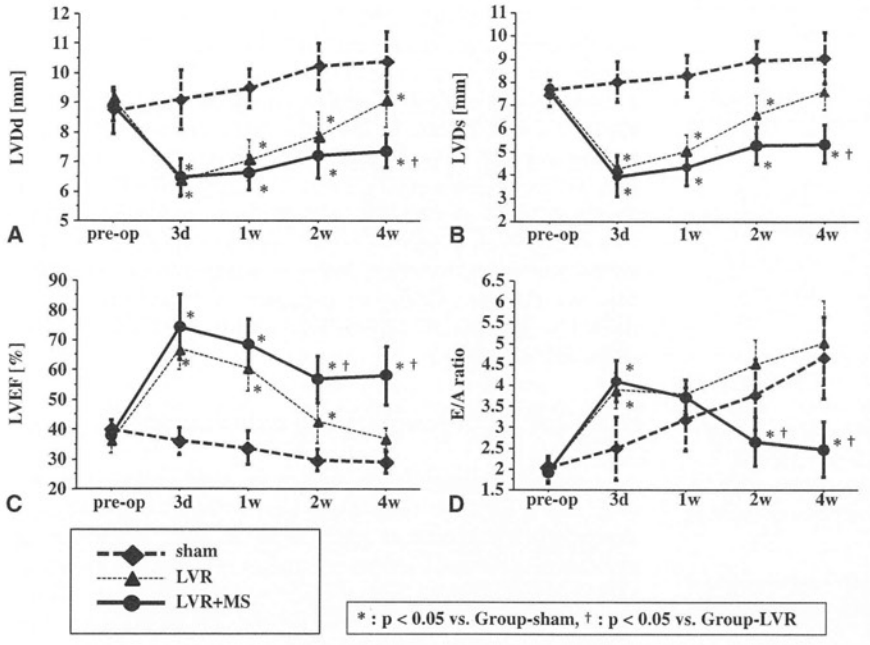

FIGURE 1. Serial echocardiographic study revealed significant decrease in left ventricular chamber size and significant increase in left ventricular ejection fraction by left ventricular restoration (LVR) in group LVR and in group LVR+ myoblast sheets (MS). However, gradual redilatation of left ventricular chamber and decrease of ejection fraction was observed in group LVR. Those later deteriorations were prevented in group LVR+MS, and the differences in chamber size and ejection fraction were significant between group LVR and group LVR+ MS 4 weeks after the operation. Changes in echocardiographic parameters before and after the operation. (A) Left ventricular dimension at end-diastole (LVDd), (B) left ventricular dimension at end-systole (LVDs), (C) Left ventricular ejection fraction (LVEF), (D) mitral valve E/A ratio. *P0.05 vs. group sham; †P0.05 vs. group LVR.

However, impairment of diastolic function and late remodeling are great concerns after LVR for ischemic cardiomyopathy (*5–7*), and the long-term effect of LVR is still controversial. Although LVR that is performed together with coronary artery bypass grafting (CABG) has been suggested to reduce the rate of hospitalization and improve ventricular function to a greater degree than CABG alone on the basis of a small, nonrandomized, case-control study (*8*), recently conducted multicenter, nonblinded, randomized trial (the Surgical Treatment for Ischemic Heart Failure [STICH] trial) have revealed that LVR does not improve the symptoms, exercise tolerance, rate of death, or hospitalization in patients with ischemic heart disease and severe LV dysfunction compared with CABG alone (*5*).

On the other hand, cell transplantation into impaired myocardium, also known as cellular cardiomyoplasty, has been investigated (*9, 10*). Recently, we have developed a new cell delivery method by the means of cell sheet, in which autologous skeletal myoblasts were transplanted in sheet form, and reported that this method was effective especially in the attenuation of LV dilatation and the improvement of LV diastolic function (*11–14*). On the basis of these findings, we hypothesized that skeletal myoblast sheet (MS) implantation may attenuate the disadvantageous effects and enhance the advantageous effects of LVR. Using a rat model of chronic myocardial infarction model, we investigated whether MS implantation combined with LVR can attenuate the redilatation and diastolic dysfunction of LV after LVR.

RESULTS

Changes in Cardiac Function by LVR and LVR Combined With MS

Two weeks after left anterior descending coronary artery (LAD) ligation, severe dilatation of the LV chamber and severe asynergy of the anterior wall were observed in all the rats. By excluding the large akinetic or dyskinetic area of the LV anterior wall, LV dimension at end-diastole (LVDd) and end-systole (LVDs) significantly decreased and left ventricular ejection fraction (LVEF) significantly increased in group LVR and in group LVR+MS 3 days after treatment (Fig. 1). However, gradual LV redilatation and decrease of LVEF were observed in group LVR. MS implantation combined with LVR attenuated those later deteriorations of LV function significantly in group LVR+MS (Fig. 1). Mitral valve *E/A* ratio showed significant restrictive pattern after LVR. In group LVR, the restrictive pattern progressed even further with time. However, addition of the MS implantation attenuated the progression of the restrictive pattern (Fig. 1).

Hemodynamic Improvement by LVR Combined With MS

Table 1 shows the results of the hemodynamic study by cardiac catheterization 4 weeks after the second operation. The basic hemodynamic indices revealed that LV end-diastolic pressure (EDP) and the time constant of isovolumic relaxation (τ) were significantly lower in group LVR+MS than in group LVR or group sham. Load-independent parameters measured by pressure-volume loop analysis revealed that end-systolic pressure (ESP) volume relationship was significantly higher in group LVR+MS than in the other two groups. EDP volume relationship (EDPVR) was significantly lower in group LVR+MS than in the other two groups.

Histological Impact of the MS on the Failing Heart

Figure 2 shows the typical cross section of the whole hearts 4 weeks after the operation from each group. Severe dilatation of the LV chamber and thinning of the LV wall were observed in group sham (Fig. 2A). In group LVR, although infracted area was excluded and smaller than that in group sham, LV chamber was markedly dilated (Fig. 2B). Also severe dilatation of the right ventricular chamber was observed. In group LVR+MS, the size of the LV chamber and the thickness of the LV wall were well preserved compared

TABLE 1. Hemodynamic indices 4 weeks after the operation

Group	Sham	LVR	LVR+MS
Basic hemodynamic indices			
HR (bpm)	219 ± 37	206 ± 20	231 ± 32
ESP (mm Hg)	60.9 ± 7.7	63.0 ± 13.9	73.0 ± 11.3[a]
EDP (mm Hg)	5.1 ± 2.2	9.0 ± 6.6	2.0 ± 1.0[a,b]
τ (msec)	21.3 ± 2.4	19.8 ± 2.2	14.4 ± 1.2[a,b]
Load independent parameters analyzed by pressure-volume loop			
ESPVR (mm Hg/ml)	1896 ± 906	1364 ± 661	4722 ± 2416[a,b]
EDPVR (/ml)	50 ± 36	42 ± 23	13 ± 6[a,b]
PRSW (mm Hg)	37.1 ± 24.3	33.0 ± 24.2	45.2 ± 32.7

[a] $P < 0.05$ vs. group sham.
[b] $P < 0.05$ vs. Group-LVR.
HR, heart rate; ESP, end-systolic pressure; EDP, end-diastolic pressure; τ, time constant of isovolumic relaxation; ESPVR, end-systolic pressure-volume relationship; EDPVR, end-diastolic pressure-volume relationship; PRSW, preload-recruitable stroke work.

with the other groups (Fig. 2C). The LV wall thickness was significantly larger in group LVR+MS than in the other two groups (vs. group sham and group LVR, $P<0.05$) (Fig. 3A). The degree of cardiac fibrosis was significantly smaller in group LVR+MS than in the other two groups (vs. group sham and group LVR, $P<0.05$) (Figs. 3B and 4A–C). Myocyte size was also significantly smaller in group LVR+MS than in the other two groups (vs. group sham and group LVR, $P<0.05$) (Figs. 3C and 4D–F). Vascular density of the LV lateral wall, the area where MS were applied in group LVR+MS, was significantly higher in group LVR+MS than in the other two groups (vs. group sham and group LVR, $P<0.05$) (Figs. 3D and 4G–I).

Suppression of Probrotic Agent Gene Expression by MS

Reverse transcription polymerase chain reaction analysis 4 weeks after the second operation revealed significantly suppressed expression of the profibrotic gene transforming growth factor-beta (TGF-β), Smad2, and reversion-inducing cysteine-rich protein with Kazal motifs (RECK) in group LVR+MS than in the other two groups (vs. group sham and group LVR, $P<0.05$) (Fig. 5A–C).

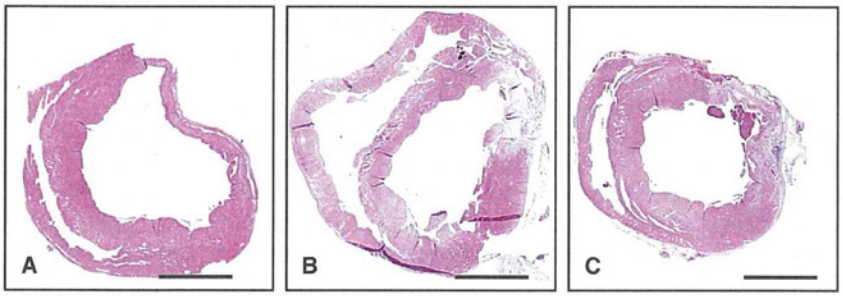

FIGURE 2. Cross section of the whole hearts 4 weeks after the operation from each group (hematoxylin-eosin staining). (A) group sham, (B) group LVR, (C) group LVR + MS.

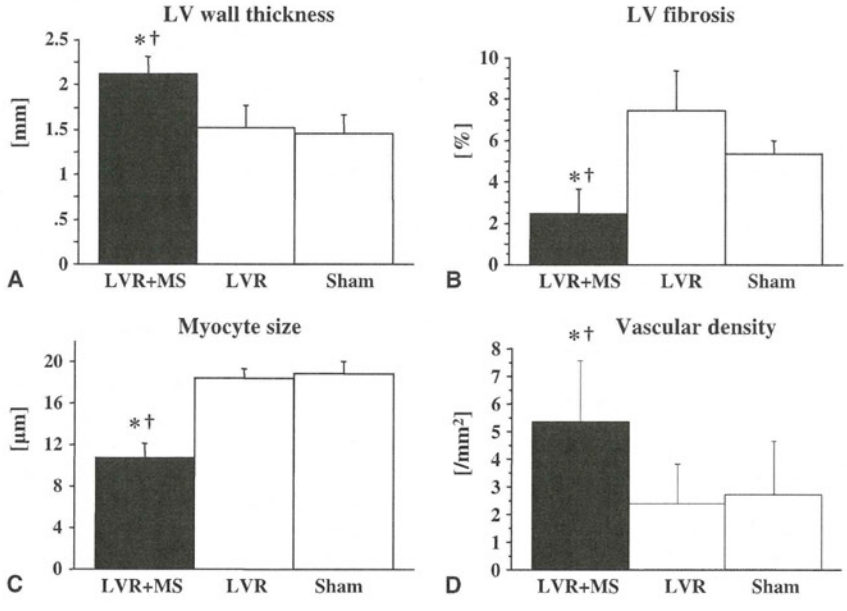

FIGURE 3. The left ventricular (LV) wall thickness was significantly larger in group left ventricular restoration (LVR)+myoblast sheets (MS) than in the other two groups 4 weeks after the operation (A). The degree of cardiac fibrosis (B) and myocyte size (C) were also significantly smaller in group LVR+MS than in the other two groups. The vascular density in the LV lateral wall, where MS were applied in group LVR+MS, were significantly higher in group LVR+MS than in the other two groups (D).

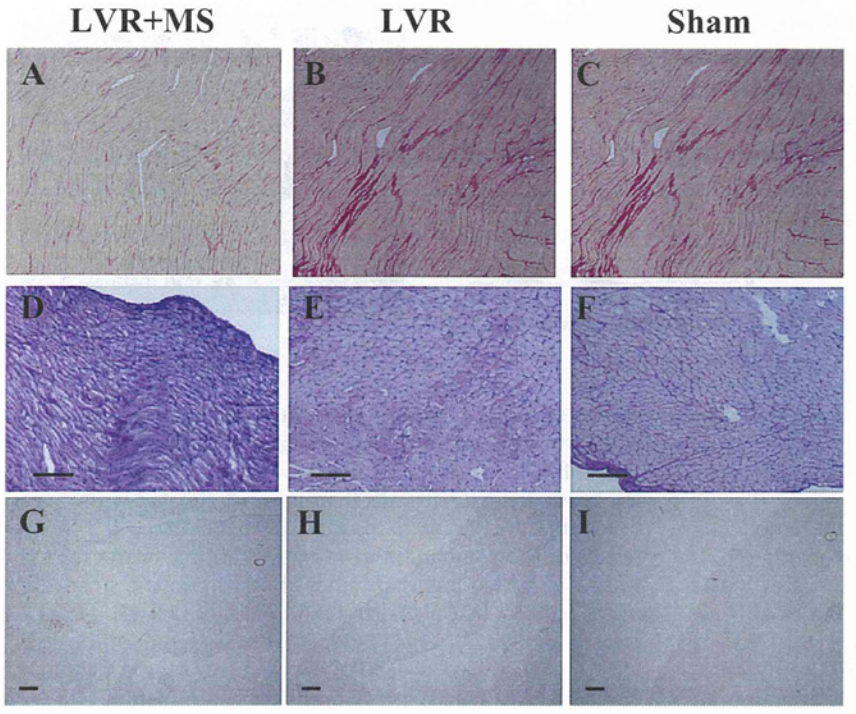

FIGURE 4. Picrosirius-red staining of myocardium from noninfarcted regions (A, B, C) and periodic acid-Schiff-stained myocardium from noninfarcted regions (D, E, F, bar=200 μm). Picrosirius-red staining of myocardium from noninfarcted regions. Sections of myocardium stained with antibody to von Willebrand factor (G, H, I, bar=300 μm).

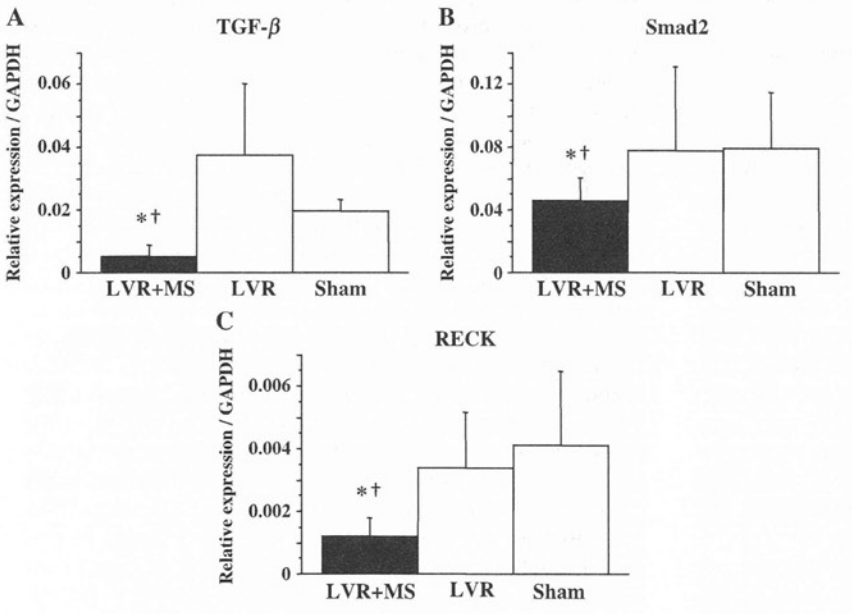

FIGURE 5. Reverse transcription polymerase chain reaction (RT-PCR) analysis 4 weeks after the second operation revealed significantly suppressed expression of the profibrotic gene transforming growth factor-beta (TGF-β) (A), Smad2 (B), and RECK (C) in group left ventricular restoration (LVR)+myoblast sheets (MS) than in the other two groups.

Engrafted Cell Survival

To evaluate the survival of engrafted cell on the recipient LV, MS made from male rats were implanted on the female LV, and surviving cell numbers were examined by detecting the Y chromosome-specific and gender consensus genes. To confirm the accuracy of the measurements, MS made from known numbers of male myoblasts were implanted on the LV wall of a female rat ex vivo, and a standard curve was prepared to determine the ratio of male cells to female cells and the relationship to the number of male cells. The correlation coefficient for the standard curve was 0.9716, indicating a significant correlation. The number of surviving engrafted cells was calculated using this standard curve (*15*). The number of cells detected on the day of implantation was approximately 64% of the engrafted cells (five layers of MS, with 3.0×10^6 myoblasts in each sheet). Surviving cells decreased to 69% of those in day 0. Although the number continued to decrease with time, 13% of those cells were still surviving on the LV wall 4 weeks after MS implantation (Fig. 6A).

Immunostaining of the green fluorescent protein (GFP) revealed that myoblasts sheets made from GFP transgenic rats

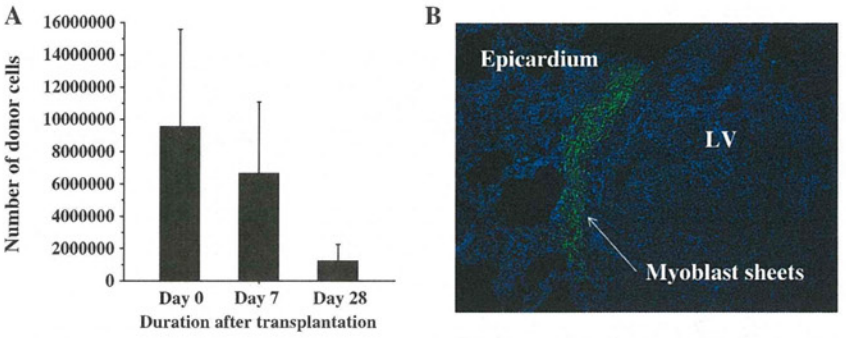

FIGURE 6. Survival of donor cells in recipient hearts. (A) Number of surviving engrafted cells in recipient hearts. Although the number of donor cells decreased with time, the surviving engrafted cells were still detectable 28 days after transplantation. (B) Immunostaining of the green fluorescent protein. Transplanted myoblast sheets were still detectable 28 days after the surgery.

were still detectable on the epicardium of LV wall 28 days after implantation (Fig. 6B).

DISCUSSION

Impairment of diastolic function and late remodeling are concerns after LVR for ischemic cardiomyopathy (*5–7*). Dor et al. (*6*) have reported the late redilatation of LV after LVR in their clinical experiences, and Nishina et al. (*16*) have developed a rat model that reproduces this clinical situation, in which model an infracted area of the LV anterior wall was simply plicated. Although LV configuration and function improved after the operation, LV chamber gradually redilated and LV function decreased, and the initial improvement almost disappeared in 4 weeks.

Using this same model, we implanted the skeletal MS concomitantly with LVR to investigate the ability of MS to overcome the drawbacks of the LVR. In this study, MS implantation attenuated the LV redilatation and decrease in EF after LVR. It was also shown by echocardiographic study and pressure-volume loop analysis that MS attenuated the impairment of diastolic function after LVR. Histological examination revealed that MS induced the angiogenesis in the myocardium where they were applied, and decreased the degree of myocardial fibrosis. MS controlled the gene expression that may regulate the myocardial fibrosis (TGF-β, Smad2, and RECK), and suppressed myocardial fibrosis. The number of viable myoblasts implanted on the LV wall concomitantly with LVR decreased with time, but they were still detectable on the LV wall 28 days after implantation. The surviving cells detected on the LV wall 28 days after transplantation were only 13% of those detected on the day of transplantation. However, to enhance the survivability and effectiveness of implanted cells, we have developed new additional therapy such as transfection of the gene for hepatocyte growth factor (HGF) (*17*) or omentum flap (*18*) combined with cell transplantation, and reported the efficacies of these additional therapies in the previous studies.

The mechanism of recovery of cardiac function by autologous MS are considered as combination of restoration of the LV wall by the MS, that is "girdling effect," and biological effects of the cytokines such as stromal-derived factor 1 (SDF-1), HGF, and vascular endothelial growth factor (VEGF) paracrined from sheet-shaped autologous myoblasts, that is "paracrine effect." SDF-1 is known to mobilize and recruit stem cells and leads to neovascularization (*19, 20*) and is secreted in skeletal muscle tissue (*21*). HGF is an angiogenic and antifibrotic factor (*22*), and VEGF is also a potent angiogenic factor (*23*). In the previous reports with animal models, we have demonstrated that the gene expressions of SDF-1, HGF, and VEGF were significantly higher in the hearts treated with MS than in hearts treated with myoblasts injection or with medium injection (*11, 14, 24*). As results of those enhanced gene expression, the hearts treated with MS showed higher number of hematopoietic stem cells in the treated area (*11*), greater vascularity (*11, 12, 14*), decreased cardiac fibrosis (*11–14, 24*), decreased apoptotic cells (*13*), and increased proliferative cells (*13*). Moreover, those effects were enhanced as the number of transplanted MS increased (*14*). Sekiya et al. (*14*) reported that the effect of the MS was maximally enhanced when it was implanted on the impaired myocardium in five layers, compared with three or one layer. Based on these data and experiences in our own laboratory, we chose the skeletal myoblasts as donor of cell sheets in this study, and decided the cell number and the layer number of the MS. In this study, we reconfirmed that angiogenesis was induced and fibrosis was suppressed by MS. It is considered that the angiogenesis enhanced the myocardial microcirculation and improved the myocardial ischemia, and resulted in attenuation of myocardial fibrosis and late remodeling. Instead of the well-known key factors secreted by MS such as SDF-1, HGF, and VEGF, we investigated the other signals that are known to control the degree of tissue fibrosis such as TGF-β, Smad, and RECK. TGF-β is a known profibrotic cytokine that has been demonstrated to induce cardiac fibrosis (*25*). The effect of TGF-β in the heart is primarily mediated though Smad2 phosphorylation (*26*). The TGF-β-Smad pathway seems to be involved in the activation of collagen-gene promoter sites, increasing DNA translation of collagen I. In this study, it was clearly proved that MS suppress the TGF-β-Smad pathway leading to the attenuation of cardiac fibrosis. RECK is known to be one of the inhibitors of metalloproteinases (*27*) and believed to be an important regulator of cardiac extracellular matrix. Although in this study we could not evaluate the matrix metalloproteinase (MMP) and tissue inhibitors of metalloproteinase activity, MS may activate the MMP acting through the suppression of RECK, leading to the reduction of fibrosis. It was shown for the first time that MS suppressed the degree of myocardial fibrosis by regulating those signals. The mechanisms by which MS regulate those signals remain to be investigated.

We also revealed that LV wall thickness was maintained and LV dilatation was attenuated by MS after LVR. From Laplace's law, this might have led to decrease in

LV wall stress and attenuation of the myocardial cellular hypertrophy.

In our previous study, we reported that MS increased elastin in the myocardium where the MS were implanted, and this might have contributed to the improvement in diastolic function (*14*). In this study, all the data acquired from echocardiography (mitral *E/A* ratio), catheter study (LVEDP, τ, and EDPVR), and histological study (fibrosis) revealed improvement of diastolic function by the MS.

One of the unique points of this study, compared with the previous studies with skeletal MS, was that the MS were applied to the viable area of the myocardium in this study. One of the most important mechanisms of the myocardial improvements by MS is considered paracrine effect of cytokines secreted from the skeletal myoblast. From this point of view, it is anticipated that the greater the number of the viable cells in the area of myocardium where the MS is attached, the greater the effect of the MS. This study is different from the previous studies in the point that the impaired myocardium was excluded by surgical LVR and the skeletal MS were attached to the remaining viable area of the myocardium. In the preliminary experiment of this study, we have also included the "MS only group" in the study groups. As reported in the previous studies, MS showed a certain effects and prevented the deterioration of the heart function compared with sham group. However, the comparisons between the group LVR+MS and "MS only group" were complicated because the conditions of the myocardium in which the MS were applied were different, so we excluded this group from the final design of this study.

Using the rat LVR model, other additional treatments such as administration of angiotensin-converting enzyme inhibitor (*28*), chymase inhibitor (*29*), or transplantation of fetal cardiomyocyte by needle injection (*30*) were reported to prevent the late remodeling after LVR in some extent. Not like the single medical treatments mentioned above, MS implantation affects on cardiac function by integrated pathway of angiogenesis, antifibrosis, mechanical unloading of the LV wall stress, and possibly other unknown mechanisms. MS implantation is supposed to be more effective than single medical treatment. As a cell delivery method, it is known that direct intramyocardial injection has several disadvantages, including cell loss caused by leakage of injected cells from the myocardium, poor survival of the grafted cells, myocardial damage after mechanical injury by the needle, and subsequent acute inflammation. MS implantation is a useful method to overcome these disadvantages, and we have reported the superiority of the myocardial sheets implantation to needle injection (*11–13*).

This study has some limitations. In this rat model, the area of myocardial infarction is not identical in all the rats 2 weeks after ligating the coronary artery, and thus the size of the LV and the degree of impairment of diastolic function are not identical in all the rats after LVR. Second, the surgery for excluding the infarction was carried out by imbrication stitches, and this is different from the actual procedure in the clinical setting, excision and re-sculpting of the left ventricle as described by Dor et al. (*6*). Additionally, we chose rats with large akinetic area as a myocardial infarction model and aggressively plicated this area to reproduce "the failing situation" after LVR. This situation may not be directly applied to clinical settings. However, we consider that the effectiveness of MS to attenuate impairment of diastolic function and late remodeling after LVR was shown by this model. We also recognize some limitations in our study with regard to the analysis of the mechanisms in which the MS reduce the cardiac fibrosis. Although we have demonstrated the enhanced gene expression of smad and RECK, further study is needed to analyze the level of gene expression of collagens, MMPs, and tissue inhibitors of metalloproteinases to show the activation of Smad2 and RECK protein.

In conclusion, skeletal MS implantation attenuated the impairment of diastolic function and the late remodeling after LVR in rat myocardial infarction model. It is suggested that MS implantation may improve the long-term outcome of LVR for ischemic heart disease.

MATERIALS AND METHODS

Animal Care

All experimental procedures and protocols used in this investigation were reviewed and approved by the institutional animal care and use committee and are in accordance with the National Institutes of Health Guide for the Care and Use of Laboratory Animals (NIH Publication No. 85-23, Revised 1996).

Isolation of Myoblasts and Construction of MS

Myoblasts were isolated from the skeletal muscle of the anterior tibialis from 3-week-old male Lewis rats and cultured as previously described (*11–14*). They were dissociated from the culture dishes with trypsin-ethylenediaminetetraacetic acid and reincubated on 35-mm temperature-responsive culture dishes (UpCell, Cellseed, Tokyo, Japan) at 37°C, with cell number adjusted to 3.0×10^6 per dish. More than 70% of these cells were actin-positive and 40% to 50% were desmin-positive (*14*). After 24 hr, the dishes were incubated at 20°C for 30 min. During that time, the MS detached spontaneously to generate free-floating, monolayer cell sheets. After detachment, the area of the sheets decreased to 1.00 ± 0.05 cm^2, while the thickness increased to 100 ± 10.0 μm (*14*). For the immunostaining of the engrafted MS, myoblasts were isolated from GFP transgenic Lewis rats and made into cell sheets in the same way as described earlier.

Myocardial Infarction Model

Eight-week-old male Lewis rats were used (220–250 g; Seac Yoshitomi Ltd. Fukuoka, Japan). The rats were anesthetized with ketamine (90 mg/kg) and Xylazine (10 mg/kg), and myocardial infarction was induced by ligation of LAD under mechanical ventilation. Two weeks after the ligation, baseline cardiac functions were measured by echocardiography, and rats that fulfill the following criteria were selected for further experiment: large akinetic or dyskinetic area in the anterior wall of the LV, LVDd 9.0 ± 1.0 mm, and LVEF $35\%\pm5\%$. For the quantitative study of the engrafted cell fate, 8-week-old female Lewis rats were used and myocardial infarction model was made in the same way as described earlier.

Experimental Groups

Male rats were randomized into three groups: 15 rats underwent only rethoracotomy (group sham), 15 underwent LVR (group LVR), and 15 underwent LVR, which was immediately followed by MS implantation (group LVR+MS). In group LVR and group LVR+MS, LVR was performed as follows: three to four mattress stitches with 7-0 polypropylene sutures were placed just onto the border line between infarcted and intact myocardium, and the infarcted myocardium was excluded (*16*). In group LVR+MS, five layers of MS were attached directly to the intact myocardium without sutures subsequently to LVR. After detachment from the temperature-responsive dish, each sheet was picked up individually and applied to the surface of the heart. After 3 to 5 min, subsequent sheets were applied and a total of five layers of MS were implanted. All the female rats underwent implantation of MS made from male rats concomitantly with LVR for the engrafted cell fate analysis. Additionally, three rats underwent implantation of the MS made from GFP positive

myoblasts after LVR in the same way as group LVR+MS for immunostaining of implanted MS.

Echocardiography

LV functions of all the treated rats were monitored by echocardiography at baseline (2 weeks after LAD ligation), 3 days, 1 week, 2 weeks, and 4 weeks after the second operation. Echocardiography was performed with a SONOS 5500 (Agilent Technologies, Palo Alto, CA) using a 12-MHz annular array transducer under anesthesia with inhalation of isoflurane. The hearts were imaged in short-axis 2D views at the level of the papillary muscles, and the LVDs and LVDd were determined. LVEF was calculated by Pombo's method, as EF (%)=$\{(LVDd^3-LVDs^3)/LVDd^3\}\times100$. All the echocardiographic studies were performed by a single investigator who was blinded to the treatment groups and the results were agreed by all the other investigators.

Hemodynamic Study and Data Analysis

Four weeks after the second operation, after the last echocardiographic study, all the rats were ventilated again. Re-re-thoracotomy was performed and the LV apex was dissected carefully to minimize hemorrhaging. A silk thread was placed under the inferior vena cava just above the diaphragm to change the LV preload. After a purse string suture was attached to the LV apex with 7-0 polypropylene, the conductance catheter (Unique Medical Co., Tokyo, Japan) was inserted through the LV apex toward the aortic valve along the longitudinal axis of the LV cavity and then fixed. A Miller 1.4 Fr pressure-tip catheter (SPR-719, Millar Instruments, Houston, TX) was also inserted from the LV apex and fixed. The conductance system and the pressure transducer controller (Integral 3 [VPR-1002], Unique Medical Co.) were set as previously reported (*31*). The pressure-volume loops and intracardiac electrocardiogram were monitored online, and the conductance, pressure, and intracardiac electrocardiographic signals were analyzed with Integral version 3 software (Unique Medical Co.) (*31*). Under stable hemodynamic conditions, the baseline indices were initially measured and then the pressure-volume loop was drawn during the inferior vena cava occlusion and analyzed.

The following indices were calculated as the baseline LV function: heart rate, ESP, EDP, and τ. ESP volume relationship and EDPVR were determined by pressure-volume loop analysis as load-independent measures of the LV function. All the catheter studies were performed by a single investigator who was blinded to the treatment groups and the results were agreed by all the other investigators.

Histological Study

After all measurements were finished, the rats were killed for histological study. In eight rats from each group, LV myocardial specimens were obtained and fixed with 10% buffered formalin and embedded in paraffin. Hematoxylin-eosin staining was performed for the measurement of the ventricular wall thickness. The thickness of the ventricular wall was measured at two points from the LV posterior area and two points from the interventricular septum, and results were expressed as the average of the four points. Picrosirius red staining was performed to detect myocardial fibrosis. Myocardial fibrosis was expressed as percent fibrosis, the fraction of red-stained area in total myocardium, with results obtained from 10 fields per section per animal from LV lateral and posterior wall. Also periodic acid-Schiff staining was performed to examine the degree of cardiomyocyte hypertrophy. Myocyte size was determined by point-to-point perpendicular lines drawn across the cross-sectional area of the cell at the level of the nucleus. The results were expressed as the average diameter of 40 myocytes randomly selected from the LV lateral and posterior wall. To label vascular endothelial cells, so that blood vessels could be counted, immunohistochemical staining for factor VIII-related antigen was performed according to a modified protocol. We used EPOS-conjugated antibody to factor VIII-related antigen coupled with HRP (Dako EPOS Anti-Human von Willebrand Factor/HRP, Dako) as primary antibody. The stained vascular endothelial cells were counted under a light microscope. Results were expressed as the number of blood vessels/mm^2.

Measurement Probrotic Agent Gene Expression 4 Weeks After LVR and MS Implantation

In the remaining seven rats from each group, the myocardium from the LV lateral wall, the area where MS were applied in group LVR+MS, were also stored in RNAlater solution (QIAGEN, Hilden, Germany). Total RNA was extracted with the RNeasy mini kit (QIAGEN), and relative levels of RNA transcripts were measured by the real-time quantitative reverse transcription polymerase chain reaction technique using the ABI PRISM 7700 Sequence Detection System. The measurement of the mRNA expression of TGF-β, Smad2, and RECK was performed in triplicate. The results are expressed after normalization for glyceraldehydes-phosphate dehydrogenase.

Quantitative and Histological Evaluation of Engrafted Cell Survival

Intact hearts from female Lewis rats were collected, freed of the right ventricular free wall, and transplanted with MS made from known numbers (3.0×10^2, 3.0×10^3, 3.0×10^4, 3.0×10^5, 3.0×10^6, or 3.0×10^7, n=3 each) of male Lewis rats myoblast. Samples were homogenized and analyzed for the levels of *sry* and *il2*, which are Y chromosome-specific and gender consensus genes, respectively. An estimate of the fraction of donor cells was calculated as $2\times$ *sry*/*il2*$\times100$, and standard curves were constructed to determine the myoblast number from the percentage of male cells (*15*). The amount of donor myoblasts was measured on the day of MS implantation (n=5), 7 days (n=6), and 28 days (n=5) after implantation. Genomic DNA was prepared using an Allprep kit (Qiagen). Quantitative polymerase chain reaction of *sry* and *il2* was performed with 1.2 μg of DNA using Taqman universal polymerase chain reaction master mix (Applied Biosystems) according to the manufacturer's instructions and an ABI PRISM7700 sequence detection system (Applied Biosystems).

To evaluate the surviving engrafted cell histologically, five layers of MS made from myoblasts of GFP transgenic Lewis rats were implanted on the LV of Lewis rats. They were killed 28 days after the surgery.

Data Analysis

All data were expressed as the mean±standard error of mean and subjected to analysis of variance (ANOVA). Time-course data were first analyzed by using repeated-measurements two-way ANOVA, and the other numeric data were analyzed by using one-way ANOVA. If significance was found, posthoc comparisons were performed. Findings were considered significant at P less than 0.05.

REFERENCES

1. Dor V, Saab M, Coste P, et al. Left ventricular aneurysm: A new surgical approach. *Thorac Cardiovasc Surg* 1989; 37: 11.
2. Athanasuleus CL, Stanley AWH Jr, Buckberg GD. Restoration of contractile function in the enlarged left ventricle by exclusion of remodeled akinetic anterior segment: Surgical strategy, myocardial protection, and angiographic results. *J Card Surg* 1998; 13: 418.
3. Athanasuleus CL, Buckberg GD, Stanley AWH, et al. Surgical ventricular restoration in the treatment of congestive heart failure due to post-infarction ventricular dilation. *J Am Coll Cardiol* 2004; 44: 1439.
4. Menicanti L, Castelvecchio S, Ranucci M, et al. Surgical therapy for ischemic heart failure: Single-center experience with surgical anterior ventricular restoration. *J Thorac Cardiovasc Surg* 2007; 134: 433.
5. Jones RH, Velazquez EJ, Michler RE, et al. Coronary bypass surgery with or without surgical ventricular reconstruction. *N Engl J Med* 2009; 360: 1.
6. Dor V, Sabatier M, Di Donato M, et al. Efficacy of endoventricular patch plasty in large postinfarction akinetic scar and severe left ventricular dysfunction: Comparison with a series of large dyskinetic scars. *J Thorac Cardiovasc Surg* 1998; 116: 50.
7. Sinatra R, Macrina F, Braccio M, et al. Left ventricular aneurysmectomy; comparison between two techniques; early and late results. *Eur J Cardiothorac Surg* 1997; 12: 291.
8. Prucz RB, Weiss ES, Patel ND, et al. Coronary artery bypass grafting with or without surgical ventricular restoration: A comparison. *Ann Thorac Surg* 2008; 86: 806.
9. Taylor DA, Atkins BZ, Hungspreugs P, et al. Regenerating functional myocardium: Improved performance after skeletal myoblast transplantation. *Nat Med* 1998; 4: 929.
10. Orlic D, Kajstura J, Chiment S, et al. Bone marrow cells regenerate infracted myocardium. *Nature* 2001; 410: 701.
11. Memon IA, Sawa Y, Fukushima N, et al. Repair of impaired myocardium by means of implantation of engineered autologous myoblast sheets. *J Thorac Cardiovasc Surg* 2005; 130: 1333.
12. Kondoh H, Sawa Y, Miyagawa S, et al. Longer preservation of cardiac performance by sheet-shaped myoblast implantation in dilated cardiomyopathic hamsters. *Cardiovasc Res* 2006; 69: 466.

13. Hata H, Matsumiya G, Miyagawa S, et al. Grafted skeletal myoblast sheets attenuate myocardial remodeling in pacing-induced canine heart failure model. *J Thoracic Cardiovasc Surg* 2006; 132: 918.
14. Sekiya N, Matsumiya G, Miyagawa S, et al. Layered implantation of myoblast sheets attenuates adverse cardiac remodeling of the infracted heart. *J Thorac Cardiovasc Surg* 2009; 138: 985.
15. Kitagawa-Sakakida S, Tori M, Li Z, et al. Active cell migration in retransplanted rat cardiac allografts during the course of chronic rejection. *J Heart Lung Transplant* 2000; 19: 584.
16. Nishina T, Nishimura K, Yuasa S, et al. Initial effects of the left ventricular repair by placation may not last long in a rat ischemic cardiomyopathy model. *Circulation* 2001; 104: I-241.
17. Miyagawa S, Sawa Y, Taketani S, et al. Myocardial regeneration therapy for heart failure. Hepatocyte growth factor enhances the effect of cellular cardiomyoplasty. *Circulation* 2002; 105: 2556.
18. Shudo Y, Miyagawa S, Fukushima S, et al. Novel regenerative therapy using cell-sheet covered with omentum flap delivers a huge number of cells in a porcine myocardial infarction model. *J Thorac Cardiovasc Surg* 2011; 142: 1199.
19. Askari AT, Unzek S, Penn MMS, et al. Effect of stromal-cell-derived factor 1 on stem-cell homing and tissue regeneration in ischemic cardiomyopathy. *Lancet* 2003; 362: 97.
20. Miyagawa S, Roth M, Saito A, et al. Tissue-engineered cardiac constructs for cardiac repair. *Ann Thorac Surg* 2011; 91: 320.
21. Ratajczak MZ, Peier S, Janowska WA, et al. Expression of functional CXCR4 by muscle satellite cells and secretion of SDF-1 by muscle-derived fibroblasts is associated with the presence of both muscle progenitors in bone marrow and hematopoietic stem/progenitor cells in muscles. *Stem Cells* 2003; 21: 363.
22. Taniyama Y, Morishita R, Aoki M, et al. Angiogenesis and antifibrotic action by hepatocyte growth factor in cardiomyopathy. *Hypertension* 2002; 40: 47.
23. Shimizu T, Okamoto H, Chiba S, et al. VEGF-mediated angiogenesis is impaired by angiotensin type 1 receptor blockade in cardiomyopathic hamster hearts. *Cardiovasc Res* 2003; 58: 203.
24. Hoashi T, Matsumiya G, Miyagawa S, et al. Skeletal myoblast sheet transplantation improves the diastolic function of a pressure-overloaded right heart. *J Thorac Cardiovasc Surg* 2009; 138: 460.
25. Nakajima H, Nakajima HO, Salcher O, et al. Atrial but not ventricular fibrosis in mice expressing a mutant transforming growth factor-beta(1) transgene in the heart. *Circ Res* 2000; 86: 571.
26. Pokharel S, Rasoul S, Roks AJ, et al. *N*-acelyl-Ser-Asp-Lys-Pro inhibits phosphorylation of Smad2 in cardiac fibrosis. *Hypertension* 2002; 40: 155.
27. Oh J, Takahashi R, Kondo S, et al. The membrane-anchored MMP inhibitor RECK is a key regulator of extracellular matrix integrity and angiogenesis. *Cell* 2001; 107: 789.
28. Nomoto T, Nishina T, Miwa S, et al. Angiotensin-converting enzyme inhibitor helps prevent late remodeling after left ventricular aneurysm repair in rats. *Circulation* 2002; 106: I-115.
29. Kanemitsu H, Takai S, Tsuneyoshi H, et al. Chronic chymase inhibition preserves cardiac function after left ventricular repair in rats. *Eur J Cardiothorac Surg* 2008; 33: 25.
30. Sakakibara Y, Tambara K, Lu F, et al. Combined procedure of surgical repair and cell transplantation for left ventricular aneurysm: An experimental study. *Circulation* 2002; 106: I-193.
31. Sato T, Shishido T, Kawada T, et al. ESPVR of in situ rat left ventricle shows contractility-dependent curvilinearity. *Am J Physiol* 1998; 274: 1429.

Send Orders of Reprints at bspsaif@emirates.net.ae

Current Pharmaceutical Biotechnology, 2013, *14*, 61-66

Cell Sheet Technology for Heart Failure

Yoshiki Sawa[1,*] and Shigeru Miyagawa[1]

Department of Cardiovascular Surgery, Osaka University Graduate School of Medicine, Osaka, Japan

Abstract: Heart failure is a life threatening disorder in worldwide and many papers reported about myocardial regeneration through surgical method induced by LVAD, cellular cardiomyoplasty (cell injection), tissue cardiomyoplasty (bioengineered cardiac graft implantation), in situ engineering (scaffold implantation), and LV restrictive devices. Some of these innovated technologies have been introduced to clinical settings. This review article provides summary about recent basical and clinical advances about myocardial regeneration induced by bioengineered cardiac tissue.

Keywords: Cells, heart failure, tissue engineering, myocardial regeneration.

1. INTRODUCTION

Recently, remarkable progress has been made in myocardial regeneration therapy, particularly in the area of cellular cardiomyoplasty, which has already been tested as a heart-failure treatment in clinical trials, using skeletal myoblasts [1] or bone marrow mononuclear cells (BM-MNCs) [2]. Although these trials demonstrated this technique's feasibility and safety, its efficacy appeared to be insufficient to repair badly damaged myocardium. Thus, a next-generation strategy in myocardial regeneration therapy, tissue-engineered cardiomyoplasty, which uses cell sheets, is being developed in the laboratory and the clinic.

This review summarizes recent advances in myocardial regeneration induced by cell sheet technology.

2. THE DEVELOPMENT OF CELL SHEET TECHNOLOGY

Okano *et al.* developed the cell sheet technique for preparing biological grafts [3], which has since been applied to several diseased organs, such as the heart [4], eye [5], and kidney [6], in the laboratory and the clinic. Cell sheets are prepared on special dishes that are coated with a temperature-responsive polymer, poly(N-isopropylacrylamide) (PIPAAm), which changes from being hydrophobic to hydrophilic when the temperature is lowered. This change releases the cell sheet, allowing it to be removed without destroying the cell-cell or cell-extra cellular matrix (ECM) interactions in the cell sheet. The greatest advantage of this technique is that the cell sheet is made only of cells, and the ECM is produced by the cells themselves, without an artificial scaffold [7]. Such cell sheets integrate well with native tissues, because of the adhesion molecules on its surface have been preserved [8].

Shimizu *et al.* developed a contractile chick cardiomyocyte sheet that had a recognizable heart tissue-like structure and showed electrical pulsatile amplitude without enzymatic or EDTA treatment in a special dish [9]. This group layered one-cell sheets to make bilayer cell sheets (an electrically communicative three-dimensional cardiac construct), which showed spontaneous and synchronous pulsation; they also showed that the cell sheets rapidly adhered together, and established linkages with desmosomes and intercalated disks [10]. A four-layered neonatal rat cardiomyocyte sheet was also developed. In this construct, the individual sheets communicate with electrical signals via connexin43. After being implanted subcutaneously, this pulsatile cardiac tissue survived for up to one year and showed spontaneous beating, a heart tissue-like structure, neovascularization, and increases in its size, conduction velocity, and contractile force, in proportion to the host growth [11, 12]. Cardiomyocyte sheets are flexible and their shape is easily changed. Artificial myocardial tubes that can produce pressure and follow the Starling mechanism have also been reported [13]. Sekine *et al.* wrapped a myocardial tube around the rat thoracic aorta and showed that the tube could produce pressure *in vivo* [14].

Interestingly, the electrical coupling between two layered sheets begins approximately 34 minutes after layering and is completed in about 46 minutes after layering, as determined by a multiple-electrode extra cellular recording system. A histological examination revealed the presence of connexin43 within 30 minutes [15]. These data predicted that the electrical coupling between a cardiomyocyte sheet and host myocardium should occur within 1 hour of implantation. Miyagawa *et al.* demonstrated that a neonatal cardiomyocyte sheet can survive in infarcted myocardium and communicate electrically with the host myocardium, as indicated by the presence of connexin43 and changes in the QRS wave and action potential amplitude. Implantation of such sheetsled to improved cardiac performance [4]. Another paper similarly showed electrical integration between a neonatal myocyte sheet and the host heart by electrophysiology [16]. Moreover, functional gap junctions and morphological integration via "bridging cardiomyocytes" between the sheet and host myocardium were detected [17]. These *in vitro* and *in vivo* studies clearly showed electrical and morphological

*Address correspondence to this author at the Department of Cardiovascular Surgery, Osaka University Graduate School of Medicine E1, 2-2 Yamadaoka, Suita, Osaka 565-0871, Japan; Tel: +81/6/6879-3154; Fax: +81/6/6879-3163; E-mail: sawa-p@surg1.med.osaka-u.ac.jp

1873-4316/13 $58.00+.00

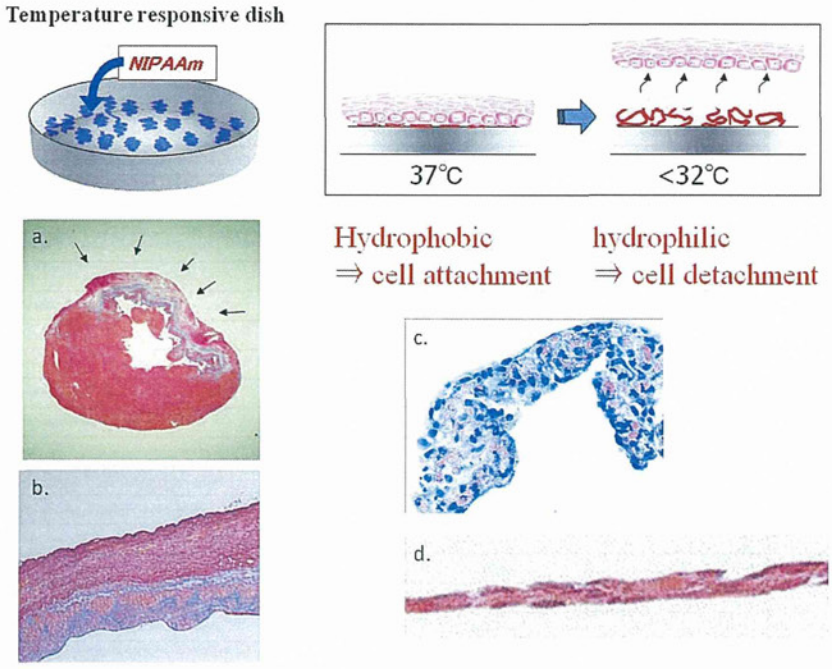

Fig. (1). How to make cell sheets?

Cell sheets can be cultured on Tempreture-responsive dishes under 37 degrees and harvested from Tempreture-responsive dishes under 22 degrees. Fig. (**1-a**, **b**) represents that myoblast sheet attached infarct area and wall thickness was well recovered. Fig. (**1-c**) showed neonatal rat cardiomyocyte sheets and Fig. (**1-d**) demonstrates rat skeletal myoblast sheets presented by HE stain [32].

coupling between the cell sheet and host myocardium, and indicated that the cell sheet may contract synchronously with the beating of the host heart and improve the regional systolic function.

Regarding the vascularization process after implantation, Sekiya *et al.* reported that the cardiomyocyte sheet expresses potential angiogenic factors, such as angiogenesis-related genes, and exhibits an endothelial cell network. Interestingly, the vasculature in layered cardiomyocyte sheets arise in the sheet itself. The vessels extend from the sheet to the host myocardium and connect with the host vasculature [18]. Another important paper showed that additional angiogenic factors, such as endothelial cells and some angiogenic growth factors, enhance angiogenesis to improve the survival of thick-layered cardiomyocyte sheets in the damaged myocardium [19]. In a study based on this paper, Sekine *et al.* reported that a cocultured sheet of neonatal cardiomyocytes and endothelial cells improved cardiac performance over that obtained with the original cardiomyocyte-only sheet, and showed enhanced vascularization [20]. These techniques, which were designed to enhance angiogenesis, may represent a breakthrough for enabling thick-layered cardiomyocyte sheets incubated in ectopic tissue to integrate successfully with damaged myocardium.

3. FROM BENCH TO BEDSIDE: STUDIES USING-MYOBLAST SHEETS

3.1. Properties of Implanted Skeletal Myoblasts

Unlike heart muscle, skeletal muscle has its own regenerative system. As soon as skeletal muscle fibers are injured, myoblasts residing under the basal membrane of the skeletal muscle fibers are mobilized and fuse with neighboring myoblasts, leading to regenerated, functional skeletal muscle. To exploit the myoblasts' self-regenerative capacity, researchers implanted these cells into distressed myocardium, which has no regenerative system. The viability of the transferred myoblasts and their affinity for the myocardium were studied, and many experiments on the myoblasts' survival, differentiation into cardiomyocytes, and electrical coupling with recipient myocytes were performed to examine the effectiveness of their implantation.

Myoblasts engrafted into cryoinjured dog myocardium [21, 22] prevented LV remodeling and improved cardiac performance [23, 24]. The implanted myoblasts did not transdifferentiate into cardiomyocytes, showing instead a mature skeletal muscle phenotype [25]. The mature skeletal muscle grafts in the distressed myocardium did not contain connexin43 or N-cadherin, indicating that they did not undergo electrical coupling with the host myocardium *in vivo* [26]. However, a low incidence of myoblast fusion with cardiomyocytes was observed [27], and a small number of these fused cells expressed connexin43 [28]. Suzuki *et al.* reported that connexin43-overexpressing myoblasts formed functional gap junctions, suggesting that myocytes have the potential to undergo synchronous contraction with host myocytes [29]. However, implanted myoblasts isolated from the recipient myocardium did not contract synchronously with host cardiomyocytes [30]. Myoblasts are thought to be the best candidate for cardiomyogenesis in the clinical setting, because cardiomyocytes cannot be cultured for clinical use, and only

Table 1. Summary of Experiments of Cell Sheet

Author	Year	Cell source	vitro/vivo	Results
Shimizu T.	2001	Chick cardiomyocytes	vitro	Spontaneous beating, heart like tissue
Shimizu T.	2002	neonatal rat cardiomyocytes	vitro	spontaneous and synchronous pulsation between cell sheets
				hitological integration of layered cell sheet
Shimizu T.	2002, 2006	neonatal rat cardiomyocytes	vitro	four layered cell sheet with electrical communication via connexin 43
				four layered cell sheet survived on the subcutaneous tissue of rat
Kubo H.	2007	neonatal rat cardiomyocytes	vitro	Artificial myocardial tube using cardiomyocyte sheet
Sekine H.	2006	neonatal rat cardiomyocytes	vivo	Myocardial tube functioned in rat abdominal aorta
Haraguchi Y.	2006	neonatal rat cardiomyocytes	vitro	Rapid electrical coupling between cell sheets
Furuta A.	2006	neonatal rat cardiomyocytes	vivo, rat	electrical coupling between cell sheet and recipient myocardium
Miyagawa S.	2005	neonatal rat cardiomyocytes	vivo, rat OMI	cell sheet survived on the rat ischemic myocrdium
				Improvement of cardiac performance
Sekine H.	2006	neonatal rat cardiomyocytes	vivo, rat	hitological integration of cell sheet with recipient myocardium
Sekiya S.	2006	neonatal rat cardiomyocytes	vivo, rat	Angiogenic potential of implanted cell sheet
Sekine H.	2008	neonatal rat cardiomyocytes	vivo, rat OMI	Endothelial cells enhanced therapeutic potential of cell sheet
		endothelial cells		
Memon IA.	2005	myoblasts	vivo, rat OMI	myoblast sheet survived on ischemic myocardium
				Improvement of cardiac performance by paracrine effect of cytokines
Kondoh H.	2006	myoblasts	vivo, DCM hamster	myoblast sheet survived on DCM hamster
				Improvement of cardiac performance and prolongation of survival rate
Hata H.	2006	myoblasts	vivo, DCM canine	Improvement of cardiac performance in preclinical study
Miyahara Y.	2006	fat derived mecenchymal stem cells	vivo, rat OMI	self-incubated in vivo and Improvement of cardiac performance on rat OMI
Kobayashi H.	2008	fibroblast and endothelial progenitor cells	vivo, rat OMI	Improvement of cardiac performance with angiogenic potential
Hobo K.	2008	finbroblast, human smooth muscle cells	vivo, rat OMI	Improvement of cardiac performance with angiogenic potential
Matsuura	2009	Sca-1 positive cells	vivo, mouse AMI	Improvement of cardiac performance via soluble VCAM-1

myoblasts can differentiate into muscle. However, implanted myoblasts can be electrically isolated from the host myocardium *in vivo*, indicating that they do not differentiate, and that the resulting cardiomyogenesis in the failing heart is quite incomplete.

3.2. Experimental Analysis of Myoblast Sheets

Cellular cardiomyoplasty is reported to have clinical regenerative potential, and a method using skeletal myoblasts has been tested in clinical trials and found relatively feasible and safe [31]. For tissue cardiomyoplasty, skeletal myoblasts are the cell source closest to being ready for use in clinical applications. Memon *et al.* demonstrated that the non-ligature implantation of a skeletal myoblast sheet into a rat cardiac ligation model regenerated the damaged myocardium and improved global cardiac function, by attenuating cardiac remodeling via hematopoietic stem-cell recruitment and growth-factor release. Moreover, this cell-delivery system by cell-sheet implantation showed better restoration of the damaged myocardium than implantation by needle injection [32].

In another study, the application of a skeletal myoblast sheet to a dilated cardiomyopathy hamster model resulted in the recovery of deteriorated myocardium, accompanied by the preservation of alpha-sarcoglycan and beta-sarcoglycan expression on the host myocytes and the inhibition of fibrosis [33]. This group implanted the myoblast sheets into 27-week-old DCM hamsters, which were at a moderate heart-failure stage (fractional shortening 16%), and showed preservation of cardiac function and histology along with prolonged survival. In addition, the grafting of skeletal myoblast sheets attenuated cardiac remodeling and improved cardiac performance in a pacing-induced canine heart-failure model [34]. These papers demonstrate that the skeletal myoblast sheet can regenerate the deteriorated myocardium induced by coronary artery diseases and DCM, in both small and large animal models. However, the only large animal study to date was the one descried above using dogs, and none has investigated the long-term results after cell-sheet implantation. Moreover, although these results indicate that skeletal myoblast sheets have potential as a treatment for moderate heart failure, its efficacy for end-stage heart failure is unknown and requires further study.

The mechanism of recovery of the damaged myocardium has not been completely elucidated, and it may be very complicated. Although Miyagawa *et al.* revealed that cytokine release and hematopoietic stem-cell recruitment are possible mechanisms of regeneration [19], other mechanisms are also likely to be involved. For example, structural proteins may be restored due to the relief of myocyte stretch, as evidenced by a reduction in the left ventricle dimension, or due to an increase in growth factors. Skeletal myoblasts cannot beat in synchrony with the host myocardium *in vitro* [35] or *in vivo* [30]. However, after myoblast sheet implantation, diastolic dysfunction in a distressed region of the myocardium recovered significantly (from our human and porcine studies, data not shown), leading to improve systolic function in the same region without contraction of the implanted myoblasts. The improvement in diastolic function may depend on the elasticity of the new scar tissue that is formed by the transplanted skeletal myoblast sheet and migrated cells. Massive angiogenesis in the implanted region is a critical characteristic for the improvement of cardiac function, and we speculate that angiogenesis and the recovery of diastolic function are major components of the regenerative mechanism of implanted myoblast sheets.

3.3. Clinical Application of Autologous Myoblast Sheets

We recently showed that implanting myoblast sheets into a human patient with end-stage heart failure caused by dilated cardiomyopathy (DCM)who was under left ventricular assist device (LVAD) support resulted in a significant improvement of cardiac performance and proved to be the bridge to his recovery. The patient was a56-year-old man suffering from idiopathic DCM, who was referred to our hospital under intra aortic balloon pumping (IABP) support, oxygenation with a respirator, portable cardiopulmonary bypass, and continuous venovenoushemodiafiltration (CVV HD). On the day of admission to our hospital, he had undergone the implantation of an extracorporeal pneumaticLVAD (Toyobo, Tokyo, Japan) and right ventricular assist system (RVAS) with extracorporeal membrane oxygenation (ECMO) using a centrifugal pump. An off-pump examination revealed that he could not be weaned from the LVAD.

Myoblast-cell-sheet transplantation into human patients was approved by the Ethical Committee and Internal Review Board of Osaka University. After the patient gave us his informed consent, an approximately 10-g piece of skeletal muscle was excised from his medial vastus muscle under general anesthesia. The isolated autologous myoblasts were seeded onto temperature-responsive culture dishes, and 20 pieces of autologous myoblast cell sheet were transplanted onto the anterior to lateral surface of the patient's dilated heart through a left lateral thoracotomy.

Off-pump tests performed at 8weeks and 3months after the transplantation showed that the ejection fraction improved from 26% to 46%, and the left ventricle dilated dimension (LVDd)increased from 49mm to 53mm. Three months after the myoblast cell-sheet transplantation, the LVAD was explanted. After the cell-sheet transplantation and LVAD removal, a Holtercardiogram demonstrated that no life-threatening arrhythmia had occurred.

This clinical research program is now ongoing in DCM and ischemic cardiomyopathy (ICM) patients both with and without LVAD.

4. OTHER KINDS OF CELL SHEETS

Some reports describe other kinds of cell sheets as being effective for improving cardiac performance. The growth of a mesenchymal stem cell (MSC) sheet on infarcted myocardium improved the anterior wall thickness, with the formation of new vessels and some differentiation of the implanted cells into cardiomyocytes [36]. The incidence of differentiation from MSCs to cardiomyocytes was low, indicating that the differentiated cardiomyocytes may not have contributed to the observed improvement in systolic function. However, in their study, the cell sheet was self-incubated *in vivo* to obtain a thick-layered sheet. Although an MSC sheet of maximum thickness, approximately 600 μm, is not strong enough to correct human end-stage heart failure [37], this method of self-incubation *in vivo* is a potentially effective strategy for creating a thick-layered sheet.

A cell sheet composed of two types of cocultured cells, fibroblasts and endothelial progenitor cells, was developed to enhance angiogenesis [20, 38]. This cocultured cell sheet enhanced blood-vessel formation and led to functional improvement [38]. Another cocultured cell sheet that combined fibroblasts and human smooth muscle cells accelerated the secretion of angiogenic factors *in vitro* and increased blood perfusion *in vivo* by the formation of new vessels [39]. This enhanced effectiveness attained by coculturing two cell types is supported by another study in which the co-implantation of BMCs and myoblasts showed improved results over the transplantation of a single cell type in a canine model of ischemic cardiomyopathy [40]. These findings have led to studies examining how the characteristics of cell sheets in the coculture method enhance their effectiveness over that of cell sheets derived from one kind of cell.

Matsuura *et al.* demonstrated that sca-1 positive cell sheet could improve cardiac performance via soluble VCAM-1and differentiation to cardiomyocytes [41]. We have already reported that myoblast sheet might improve cardiac performance via cytokines such as HGF or VEGF. So the mechanisms of improvement of cardiac performance might be different according to cell source, and we must check which cell sources are most effective for the treatment of heart failure.

5. ADVANTAGES OF THE CELL SHEET TECHNIQUE

The proportion of injected cells surviving to engraft the infarcted myocardium is too low to be effective; this low engraftment may be caused by the injected cells leaking out of the injected region, being carried to other organs, or losing their function due to mechanical stress. The resulting rapid cell loss [32] severely limits the usefulness of this myoblast cell therapy.

To overcome the problems associated with the intramyocardial injection of cells, also includes a limited graft area, investigators have combined cell transplantation with protein or gene therapy [19], or with tissue-engineering techniques [4]. We also developed a new cell-delivery system that uses tissue-engineered myoblast grafts grown as cell sheets, and we have performed animal investigations to guide clinical trials. These studies showed that the viability of these transplanted cells was high compared with that of injected cells; myoblasts survived for at least 3 months in the heart tissue of aporcine model of heart failure treated with autologous myoblast sheets [32]. Using tissue-engineering and temperature-responsive culturing techniques, we showed that cells could be applied in larger numbers, were viable at transplantation, and were not lost from the applied region when implanted as sheets. Furthermore, cell sheets can be engrafted onto the failed myocardium and contribute to the attenuation of cardiac dysfunction and remodeling as a direct effect of the engrafted myoblasts [32].

In cell therapy for cardiac disease, life-threatening adverse events involving arrhythmogenicity area potential threat in both animal models and humans [42]; however, life-threatening arrhythmias have not been observed in the patients' clinical course after autologous cell sheet transplantation. However, arrhythmia does occur in the natural clinical course of severe heart failure, so its cause often cannot be clearly identified. Procedures using needle injection might cause scars in the myocardium, and such scars could induce arrhythmias. Our cell-delivery techniques using cell sheets prepared on temperature-responsive culture dishes might carry less risk for inducing arrhythmia. Myoblasts have a

weak electrical potential, and it might be possible for them to induce arrhythmia if they survive in the myocardium. However, cell sheets may not be able to induce arrhythmia because they are attached to the epicardium.

On the other hand, the cell sheet implantation technique has some disadvantages *in vivo*. One problem is that it is technically difficult to implant myoblast sheets into the heart, which is done while the heart is actively beating. Furthermore, sometimes the site of implantation is at an angle that causes the implanted myoblast sheet to slide downward.

Another problem is the limited blood perfusion to the implanted cell sheets. Although we have reported that cardiac performance improves with a larger number of implanted myoblast sheets, the use of too many cell sheets results in a poor blood supply. Therefore, an additional strategy, such as combining myoblasts with angiogenic factors or other types of cells to establish a vasculature network may be needed to solve this problem.

CONCLUSIONS

In this review, we surveyed many exciting advances in myocardial regeneration therapy made possible by cell sheet technology. Remarkable progress has been made in cell-based treatments, including cellular cardiomyoplasty and tissue cardiomyoplasty, in a very short period of time, and many researchers and clinicians are enthusiastic about developing new technologies and examining their mechanisms from the physiological, cellular, histological, and functional points of view, to relieve the suffering of their patients. Owing to these studies, some techniques have already been tested in clinical applications, but the mechanisms by which they improve cardiac function are still largely unknown, and much of the technology is still rudimentary, in both the lab and the clinic. However, the field of clinical myocardial regenerative therapy is still in its infancy, and we expect to see much progress in this innovate technology in the years to come.

CONFLICT OF INTEREST

The author(s) confirm that this article content has no conflicts of interest.

ACKNOWLEDGEMENTS

The author acknowledges financial support from Health and Labour Sciences Research Grants Research on Regenerative Medicine for Clinical Application and the JSPS Core-to-Core Program.

REFERENCES

[1] Menasche, P.; Alfieri, O.; Janssens, S.; McKenna, W.; Reichens purner, H.; Trinquart, L.; Vilquin, J.T.; Marolleau, J.P.; Seymour, B.; Larghero, J.; Lake, S.; Chatellier, G.; Solomon, S.; Desnos, M.; Hagege, A.A. The Myoblast Autologous Grafting in Ischemic Car diomyopathy (MAGIC) trial: first randomized placebo-controlled study of myoblast transplantation. *Circulation*,**2008**, *117*,1189-1200.

[2] Strauer, B.E.; Brehm, M.; Zeus, T.; Kostering, M.; Hernandez, A.; Sorg, R.V.; Kogler, G.; Wernet, P. Repair of infarcted myocardium by autologous intracoronary mononuclear bone marrow cell transplantation in humans. *Circulation*, **2002**, *106*,1913-1918.

[3] Okano, T.; Yamada, N.; Sakai, H.; Sakurai, Y. A novel recovery system for cultured cells using plasma-treated polystyrene dishes grafted with poly(N-isopropylacrylamide). *J. Biomed. Mater. Res.*, **1993**, *27*, 1243-1251.

[4] Miyagawa, S.; Sawa, Y.; Sakakida, S.; Taketani, S.; Kondoh, H.; Memon, I.A.; Imanishi, Y.; Shimizu, T.; Okano, T.; Matsuda, H. Tissue cardiomyoplasty using bioengineered contractile cardiomyo cyte sheets to repair damaged myocardium: their integration with recipient myocardium. *Transplantation*, **2005**, *80*, 1586-1595.

[5] Nishida, K.; Yamato, M.; Hayashida, Y.; Watanabe, K.; Yama moto, K.; Adachi, E.; Nagai, S.; Kikuchi, A.; Maeda, N.; Watanabe, H.; Okano, T.; Tano, Y. Corneal reconstruction with tissue-engineered cell sheets composed of autologous oral mucosal epithelium. *N. Engl. J. Med.*, **2004**, *351*, 1187-1196.

[6] Kushida, A.; Yamato, M.; Isoi, Y.; Kikuchi, A.; Okano, T. A noninvasive transfer system for polarized renal tubule epithelial cell sheets using temperature-responsive culture dishes. *Eur. Cell Mater.*, **2005**, *10*, 23-30 discussion 23-30.

[7] Masuda, S.; Shimizu, T.; Yamato, M.; Okano, T. Cell sheet enginee ring for heart tissue repair. *Adv. Drug Deliv. Rev.*, **2008**, *60*, 277-285.

[8] Kushida, A.; Yamato, M.; Konno, C.; Kikuchi, A.; Sakurai, Y.; Okano, T. Decrease in culture temperature releases monolayer endothelial cell sheets together with deposited fibronectin matrix from temperature-responsive culture surfaces. *J. Biomed. Mater. Res.*, **1999**, *45*, 355-362.

[9] Shimizu, T.; Yamato, M.; Kikuchi, A.; Okano, T. Two-dimensional manipulation of cardiac myocyte sheets utilizing temperature-responsive culture dishes augments the pulsatile amplitude. *Tissue Eng.*, **2001**, *7*, 141-151.

[10] Shimizu, T.; Yamato, M.; Akutsu, T.; Shibata, T.; Isoi, Y.; Kikuchi, A.; Umezu, M.; Okano, T. Electrically communicating three-dimensional cardiac tissue mimic fabricated by layered cultured cardiomyocyte sheets. *J. Biomed. Mater. Res.*, **2002**, *60*, 110-117.

[11] Shimizu, T.; Yamato, M.; Isoi, Y.; Akutsu, T.; Setomaru, T.; Abe, K.; Kikuchi, A.; Umezu, M.; Okano, T. Fabrication of pulsatile cardiac tissue grafts using a novel 3-dimensional cell sheet manipulation technique and temperature-responsive cell culture surfaces. *Circ. Res.*, **2002**, *90*, e40.

[12] Shimizu, T.; Sekine, H.; Isoi, Y.; Yamato, M.; Kikuchi, A.; Okano, T. Long-term survival and growth of pulsatile myocardial tissue grafts engineered by the layering of cardiomyocyte sheets. *Tissue Eng.*, **2006**, *12*, 499-507.

[13] Kubo, H.; Shimizu, T.; Yamato, M.; Fujimoto, T.; Okano, T. Creation of myocardial tubes using cardiomyocyte sheets and an *in vitro* cell sheet-wrapping device. *Biomaterials*, **2007**, *28*, 3508-3516.

[14] Sekine, H.; Shimizu, T.; Yang, J.; Kobayashi, E.; Okano, T. Pulsatile myocardial tubes fabricated with cell sheet engineering. *Circulation*, **2006**, *114*, 187-93.

[15] Haraguchi, Y.; Shimizu, T.; Yamato, M.; Kikuchi, A.; Okano, T. Electrical coupling of cardiomyocyte sheets occurs rapidly via functional gap junction formation. *Biomaterials*, **2006**, *27*, 4765-4774.

[16] Furuta, A.; Miyoshi, S.; Itabashi, Y.; Shimizu, T.; Kira, S.; Hayakawa, K.; Nishiyama, N.; Tanimoto, K.; Hagiwara, Y.; Satoh, T.; Fukuda, K.; Okano, T.; Ogawa, S. Pulsatile cardiac tissue grafts using a novel three-dimensional cell sheet manipulation technique functionally integrates with the host heart, *in vivo*. *Circ. Res.*, **2006**, *98*, 705-712.

[17] Sekine, H.; Shimizu, T.; Kosaka, S.; Kobayashi, E.; Okano, T. Cardiomyocyte bridging between hearts and bioengineered myocardial tissues with mesenchymal transition of mesothelial cells. *J. Heart Lung Transplant*, **2006**, *25*, 324-332.

[18] Sekiya, S.; Shimizu, T.; Yamato, M.; Kikuchi, A.; Okano, T. Bioengineered cardiac cell sheet grafts have intrinsic angiogenic potential. *Biochem. Biophys. Res. Commun.*, **2006**, *341*, 573-582.

[19] Miyagawa, S.; Sawa, Y.; Taketani, S.; Kawaguchi, N.; Nakamura, T.; Matsuura, N.; Matsuda, H. Myocardial regeneration therapy for heart failure: hepatocyte growth factor enhances the effect of cellular cardiomyoplasty. *Circulation*, **2002**, *105*, 2556-2561.

[20] Sekine, H.; Shimizu, T.; Hobo, K.; Sekiya, S.; Yang, J.; Yamato, M.; Kurosawa, H.; Kobayashi, E.; Okano, T. Endothelial cell coculture within tissue-engineered cardiomyocyte sheets enhances

neovascularization and improves cardiac function of ischemic hearts. *Circulation*, **2008**, *118*, S145-152.

[21] Marelli, D.; Desrosiers, C.; el-Alfy, M.; Kao, R.L.; Chiu, R.C. Cell transplantation for myocardial repair: an experimental approach. *Cell Transplant*, **1992**, *1*, 383-390.

[22] Chiu, R.C.; Zibaitis, A.; Kao, R.L. Cellular cardiomyoplasty: myo cardial regeneration with satellite cell implantation. *Ann. Thorac. Surg.*,**1995**, *60*, 12-18.

[23] Jain, M.; DerSimonian, H.; Brenner, D.A.; Ngoy, S.; Teller, P.; Edge, A.S.; Zawadzka, A.; Wetzel, K.; Sawyer, D.B.; Colucci, W.S.; Apstein, C.S.; Liao, R. Cell therapy attenuates deleterious ventricular remodeling and improves cardiac performance after myocardial infarction. *Circulation*, **2001**, *103*, 1920-1927.

[24] Taylor, D.A.; Atkins, B.Z.; Hungspreugs, P.; Jones, T.R.; Reedy, M.C.; Hutcheson, K.A.; Glower, D.D.; Kraus, W.E. Regenerating functional myocardium: improved performance after skeletal myoblast transplantation. *Nat. Med.*, **1998**, *4*, 929-933.

[25] Reinecke, H.; Poppa, V.; Murry, C.E. Skeletal muscle stem cells do not transdifferentiate into cardiomyocytes after cardiac grafting. *J. Mol. Cell Cardiol.*, **2002**, *34*, 241-249.

[26] Reinecke, H.; MacDonald, G.H.; Hauschka, S.D.; Murry, C.E. Electromechanical coupling between skeletal and cardiac muscle. Implications for infarct repair. *J. Cell Bio.*, **2000**, *149*, 731-740.

[27] Reinecke, H.; Minami, E.; Poppa, V.; Murry, C.E. Evidence for fusion between cardiac and skeletal muscle cells. *Circ. Res.*, **2004**, *94*, e56-60.

[28] Rubart, M.; Soonpaa, M.H.; Nakajima, H.; Field, L.J. Spontaneous and evoked intracellular calcium transients in donor-derived myocytes following intracardiac myoblast transplantation. *J. Clin. Invest.*, **2004**, *114*, 775-783.

[29] Suzuki, K.; Brand, N.J.; Allen, S.; Khan, M.A.; Farrell, A.O.; Murtuza, B.; Oakley, R.E.; Yacoub, M.H. Overexpression of connexin 43 in skeletal myoblasts: Relevance to cell transplantation to the heart. *J. Thorac. Cardiovasc. Surg.*, **2001**, *122*, 759-766.

[30] Leobon, B.; Garcin, I.; Menasche, P.; Vilquin, J.T.; Audinat, E.; Charpak, S. Myoblasts transplanted into rat infarcted myocardium are functionally isolated from their host. *Proc. Natl. Acad. Sci. USA*, **2003**, *100*, 7808-7811.

[31] Dib, N.; Michler, R.E.; Pagani, F.D.; Wright, S.; Kereiakes, D.J.; Lengerich, R.; Binkley, P.; Buchele, D.; Anand, I.; Swingen, C.; Di Carli, M.F.; Thomas, J.D.; Jaber, W.A.; Opie, S.R.; Campbell, A.; McCarthy, P.; Yeager, M.; Dilsizian, V.; Griffith, B.P.; Korn, R.; Kreuger, S.K.; Ghazoul, M.; MacLellan, W.R.; Fonarow, G.; Eisen, H.J.; Dinsmore, J.; Diethrich, E. Safety and feasibility of auto logous myoblast transplantation in patients with ischemic cardio myopathy: four-year follow-up. *Circulation*, **2005**, *112*, 1748-1755.

[32] Memon, I.A.; Sawa, Y.; Fukushima, N.; Matsumiya, G.; Miyagawa, S.; Taketani, S.; Sakakida, S.K.; Kondoh, H.; Aleshin, A.N.; Shimizu, T.; Okano, T.; Matsuda, H. Repair of impaired myocardium by means of implantation of engineered autologous myoblast sheets. *J. Thorac. Cardiovasc. Surg.*, **2005**, *130*, 1333-1341.

[33] Kondoh, H.; Sawa, Y.; Miyagawa, S.; Sakakida-Kitagawa, S.; Memon, I.A.; Kawaguchi, N.; Matsuura, N.; Shimizu, T.; Okano, T.; Matsuda, H. Longer preservation of cardiac performance by sheet-shaped myoblast implantation in dilated cardiomyopathic hamsters. *Cardiovasc. Res.*, **2006**, *69*, 466-475.

[34] Hata, H.; Matsumiya, G.; Miyagawa, S.; Kondoh, H.; Kawaguchi, N.; Matsuura, N.; Shimizu, T.; Okano, T.; Matsuda, H.; Sawa, Y. Grafted skeletal myoblast sheets attenuate myocardial remodeling in pacing-induced canine heart failure model. *J. Thorac. Cardio vasc. Surg.*, **2006**, *132*, 918-924.

[35] Itabashi, Y.; Miyoshi, S.; Yuasa, S.; Fujita, J.; Shimizu, T.; Okano, T.; Fukuda, K.; Ogawa, S. Analysis of the electrophysiological properties and arrhythmias in directly contacted skeletal and cardiac muscle cell sheets. *Cardiovasc. Res.*, **2005**, *67*, 561-570.

[36] Miyahara, Y.; Nagaya, N.; Kataoka, M.; Yanagawa, B.; Tanaka, K.; Hao, H.; Ishino, K.; Ishida, H.; Shimizu, T.; Kangawa, K.; Sano, S.; Okano, T.; Kitamura, S.; Mori, H. Monolayered mesen chymal stem cells repair scarred myocardium after myocardial infarction. *Nat. Med.*, **2006**, *12*, 459-465.

[37] Sabbah, H.N. The cardiac support device and the myosplint: treating heart failure by targeting left ventricular size and shape. *Ann. Thorac. Surg.*, **2003**, *75*, S13-19.

[38] Kobayashi, H.; Shimizu, T.; Yamato, M.; Tono, K.; Masuda, H.; Asahara, T.; Kasanuki, H.; Okano, T. Fibroblast sheets co-cultured with endothelial progenitor cells improve cardiac function of infarcted hearts. *J. Artif Organs*, **2008**, *11*, 141-147.

[39] Hobo, K.; Shimizu, T.; Sekine, H.; Shin'oka, T.; Okano, T.; Kurosawa, H. Therapeutic angiogenesis using tissue engineered human smooth muscle cell sheets. *Arterioscler. Thromb. Vasc. Biol.*, **2008**, *28*, 637-643.

[40] Memon, I.A.; Sawa, Y.; Miyagawa, S.; Taketani, S.; Matsuda, H. Combined autologous cellular cardiomyoplasty with skeletal myoblasts and bone marrow cells in canine hearts for ischemic cardiomyopathy. *J. Thorac. Cardiovasc. Surg.*, **2005**, *130*, 646-653.

[41] Matsuura, K.; Honda, A.; Nagai, T.; Fukushima, N.; Iwanaga, K.; Tokunaga, M.; Shimizu, T.; Okano, T.; Kasanuki, H.; Hagiwara, N.; Komuro, I. Transplantation of cardiac progenitor cells amelio rates cardiac dysfunction after myocardial infarction in mice. *J. Clin. Invest.*, **2009**, *119*, 204-2217.

[42] Menasche, P.; Hagege, A.A.; Vilquin, J.T.; Desnos, M.; Abergel, E.; Pouzet, B.; Bel, A.; Sarateanu, S.; Scorsin, M.; Schwartz, K.; Bruneval, P.; Benbunan, M.; Marolleau, J.P.; Duboc, D. Auto logous skeletal myoblast transplantation for severe postinfarction left ventricular dysfunction. *J. Am. Coll Cardiol.*, **2003**, *41*, 1078-1083.

Received: August 24, 2010 **Accepted: November 25, 2010**

Moriyama et al. BMC Cell Biology 2012, 13:21
http://www.biomedcentral.com/1471-2121/13/21

BMC Cell Biology

RESEARCH ARTICLE Open Access

Human adipose tissue-derived multilineage progenitor cells exposed to oxidative stress induce neurite outgrowth in PC12 cells through p38 MAPK signaling

Mariko Moriyama[1,2†], Hiroyuki Moriyama[1*†], Ayaka Ueda[1], Yusuke Nishibata[1], Hanayuki Okura[2], Akihiro Ichinose[3], Akifumi Matsuyama[2] and Takao Hayakawa[1]

Abstract

Background: Adipose tissues contain populations of pluripotent mesenchymal stem cells that also secrete various cytokines and growth factors to support repair of damaged tissues. In this study, we examined the role of oxidative stress on human adipose-derived multilineage progenitor cells (hADMPCs) in neurite outgrowth in cells of the rat pheochromocytoma cell line (PC12).

Results: We found that glutathione depletion in hADMPCs, caused by treatment with buthionine sulfoximine (BSO), resulted in the promotion of neurite outgrowth in PC12 cells through upregulation of bone morphogenetic protein 2 (BMP2) and fibroblast growth factor 2 (FGF2) transcription in, and secretion from, hADMPCs. Addition of *N*-acetylcysteine, a precursor of the intracellular antioxidant glutathione, suppressed the BSO-mediated upregulation of BMP2 and FGF2. Moreover, BSO treatment caused phosphorylation of p38 MAPK in hADMPCs. Inhibition of p38 MAPK was sufficient to suppress BMP2 and FGF2 expression, while this expression was significantly upregulated by overexpression of a constitutively active form of MKK6, which is an upstream molecule from p38 MAPK.

Conclusions: Our results clearly suggest that glutathione depletion, followed by accumulation of reactive oxygen species, stimulates the activation of p38 MAPK and subsequent expression of BMP2 and FGF2 in hADMPCs. Thus, transplantation of hADMPCs into neurodegenerative lesions such as stroke and Parkinson's disease, in which the transplanted hADMPCs are exposed to oxidative stress, can be the basis for simple and safe therapies.

Keywords: Human adipose-derived multilineage progenitor cells, Adult stem cells, Reactive oxygen species, p38 MAPK, Neurite outgrowth, BMP2, FGF2, Neurodegenerative disorders

Background

Mesenchymal stem cells (MSCs) are pluripotent stem cells that can differentiate into various types of cells [1-6]. These cells have been isolated from bone marrow [1], umbilical cord blood [2], and adipose tissue [3-6] and can be easily obtained and expanded *ex vivo* under appropriate culture conditions. Thus, MSCs are an attractive material for cell therapy and tissue engineering. Human adipose tissue-derived mesenchymal stem cells, also referred to as human adipose tissue-derived multilineage progenitor cells (hADMPCs), are especially advantageous because they can be easily and safely obtained from lipoaspirates, and the ethical issues surrounding other sources of stem cells can be avoided [4-6]. Moreover, hADMPCs have more pluripotent properties for regenerative medical applications than other stem cells, since these cells have been reported to have the ability to migrate to the injured area and differentiate into hepatocytes [4], cardiomyoblasts [5], pancreatic cells [7], and neuronal cells [8-10]. In addition, it is known that hADMPCs secrete a wide variety of cytokines and

* Correspondence: moriyama@phar.kindai.ac.jp
†Equal contributors
[1]Pharmaceutical Research and Technology Institute, Kinki University, 3-4-1 Kowakae, Higashi-Osaka, Osaka 577-8502, Japan
Full list of author information is available at the end of the article

growth factors necessary for tissue regeneration including nerve growth factor (NGF), brain-derived neurotrophic factor (BDNF), fibroblast growth factors (FGFs), vascular endothelial growth factor (VEGF) and hepatocyte growth factor (HGF) [11-14].

Recently, several groups have reported that hADMPCs facilitate neurological recovery in experimental models of stroke [9,10,15] and Parkinson's disease [16]. Despite the superiority of hADMPCs over other stem cells, the potential use of hADMPCs for the treatment of these neurodegenerative disorders has not been fully investigated. It has been reported that administration of hADMPCs in animal models of acute ischemic stroke markedly decreased brain infarct size, improved neurological function by enhancing angiogenesis and neurogenesis, and showed anti-inflammatory and anti-apoptotic effects [9,10]. These effects were due in part to increased secretion levels of VEGF, HGF and bFGF under hypoxic conditions [13], indicating the role of hADMPCs in reducing the severity of hypoxia-ischemic lesions.

In addition to hypoxic stress, ischemic lesions are generally subject to inflammation, which leads to the generation of reactive oxygen species (ROS) [17,18]. ROS are

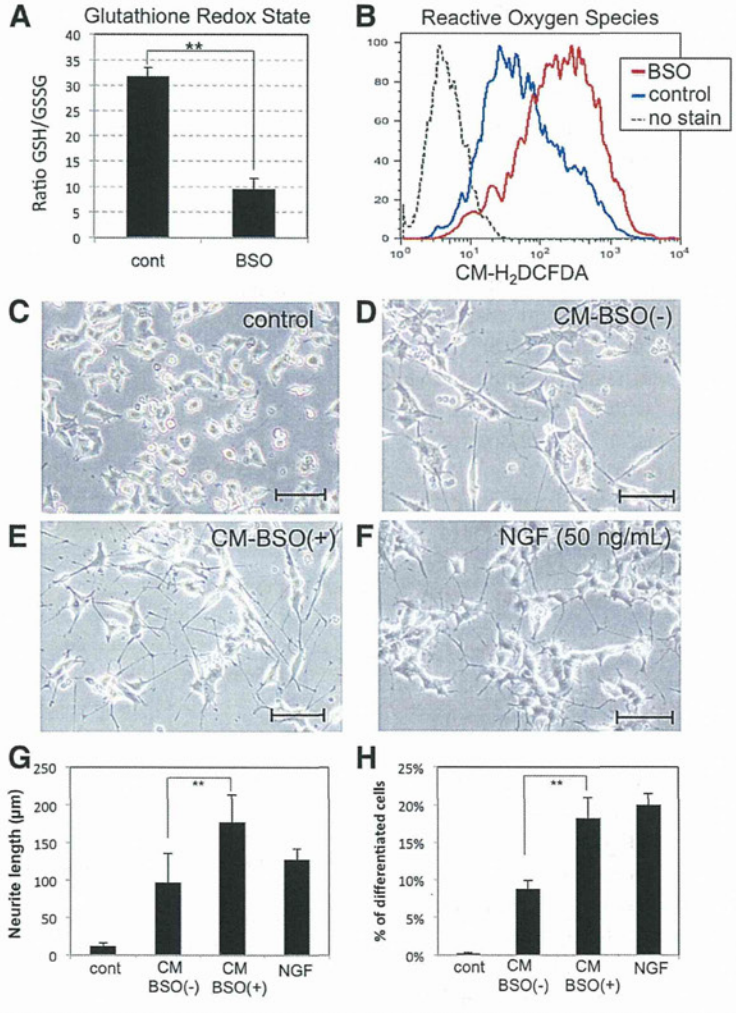

Figure 1 Conditioned medium from hADMPCs exposed to oxidative stress induces neurite outgrowth in PC12 cells. (A, B) Decrease of the reduced/oxidized glutathione ratios and increase in the intracellular ROS levels in hADMPCs treated with BSO. hADMPCs were treated with 1 mM BSO for 16 h, and cellular GSH/GSSG levels (**A**) or ROS (H_2O_2) levels (**B**) were analyzed. **(C-G)** Induction of neurite outgrowth in PC12 cells by conditioned medium from BSO-treated hADMPCs. PC12 cells were induced to differentiation by changing medium to differentiation medium alone (**C**), CM-BSO (–) (**D**), CM-BSO (+) (**E**), or differentiation medium with NGF (50 ng/mL) (**F**) for 2 days. Scale bars, 200 μm. (**G**) One hundred individual neurites were measured in each sample using Dynamic Cell Count Analyzer BZ-H1C (Keyence, Osaka, Japan) and average neurite length was calculated. **, $P < 0.01$ (Student's t test). **(H)** Percentage of neurite-bearing PC12 cells. A cell was scored positive for bearing neurites if it has a thin neurite extension that is double the length of the cell body diameter. A total of 500–600 cells in each sample were counted. **, $P < 0.01$ (Student's t test).

generated as a natural byproduct of normal aerobic metabolism, and mitochondrial respiration, together with oxidative enzymes such as plasma membrane oxidase, is considered to be the major intracellular source of ROS production [19]. Although appropriate levels of ROS play an important role in several physiological processes, oxidative damage initiated by excessive ROS causes many pathological conditions including inflammation, atherosclerosis, aging, and cancer. Neuronal cells are especially vulnerable to oxidative stress, and numerous studies have examined the crucial roles of oxidative stress in neurodegenerative disorders such as stroke [17,18], Alzheimer's disease [20,21], and Parkinson's disease [22,23]. In these diseases, microglia, the macrophages of the central nervous system (CNS), are activated in response to a local inflammation [24] and generate large amounts of reactive oxygen and nitrogen species, thereby exposing nearby neurons to stress [18,25]. Thus, the influence of oxidative stress generated by neurodegenerative lesion on hADMPCs needs to be further studied.

In this study, we examined the role of oxidative stress on hADMPCs in neurite outgrowth in cells of the rat pheochromocytoma cell line (PC12). Upon treatment with buthionine sulfoximine (BSO), an inhibitor of the rate-limiting enzyme in the synthesis of glutathione, hADMPCs accumulated ROS, which resulted in the upregulation of expression levels of the neurotrophic factors BMP2 and FGF2. Our present data thus provide new insights into understanding the mechanism of how hADMPCs exposed to oxidative stress contribute to neurogenesis, and this may explain the effects of stem cell transplantation therapy with hADMPCs in treating ischemic stroke.

Results

hADMPCs exposed to oxidative stress stimulate neurite outgrowth in PC12 cells

hADMPCs were treated with 1 mM BSO for 24 h; a group of hADMPCs that were not given any treatment was used as the control group. As shown in Figure 1A and B, BSO treatment resulted in significant reduction of intracellular reduced glutathione levels, followed by accumulation of intracellular reactive oxygen species (ROS) in hADMPCs. To investigate whether accumulation of ROS affects secretion of cytokines from hADMPCs, conditioned medium from BSO-treated (CM-BSO (+)) or BSO-untreated (CM-BSO (−)) hADMPCs was added to PC12 cells. As expected, addition of NGF significantly induced neurite outgrowth in the PC12 cells (Figure 1F, G, H). hADMPCs, like other mesenchymal stem cells derived from bone marrow or adipose tissue, may secrete many cytokines including NGF, BDNF and FGF2, and this may account for the slight induction of neurite outgrowth seen in the CM-BSO (−) treated cells (Figure 1D, G, H). In contrast, the number and length of neurite outgrowth of PC12 cells in CM-BSO (+) (Figure 1E) was markedly enhanced compared with those in CM-BSO (−) (Figure 1D, E, G, H).

Conditioned medium from BSO-treated hADMPCs activates Erk1/2 MAPK and Smad signaling in PC12 cells

To investigate which intracellular signaling pathways were involved in the neurite outgrowth of PC12 cells in CM-BSO (+), we used western blotting to determine the phosphorylation levels of Erk1/2 MAPK, p38 MAPK, Smad1/5/8 and Akt in PC12 cells in various culture conditions. NGF significantly activated Erk1/2 MAPK and Akt signaling pathway (Figure 2). In contrast, Erk1/2 MAPK was not activated in PC12 cells exposed to CM-BSO (−), while an increase in phosphorylated Smad1/5/8 was observed. Interestingly, CM-BSO (+) treatment led to both a significant increase in Smad1/5/8 phosphorylation levels as well as activation of the Erk1/2 MAPK

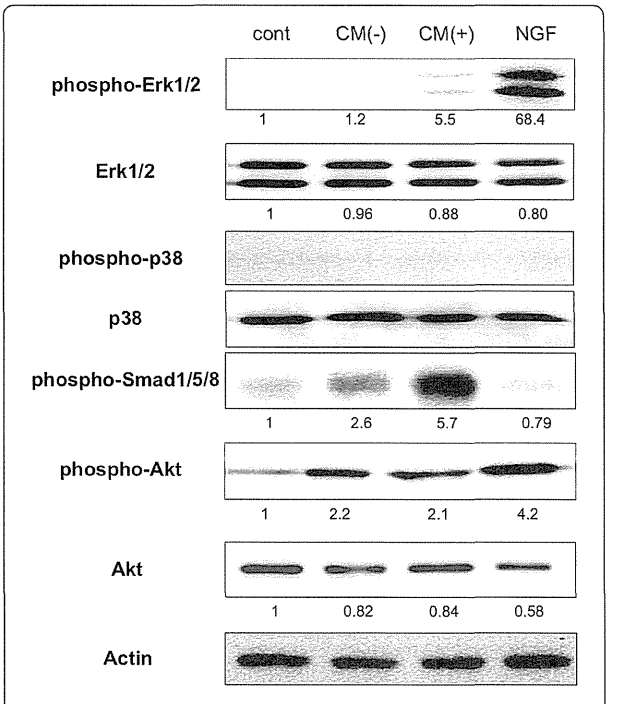

Figure 2 Erk1/2 MAPK and Smad1/5/8 are activated in PC12 cells cultured in conditioned medium from BSO-treated hADMPCs. Western blot analysis of PC12 cells cultured in differentiation medium alone (cont), CM-BSO (−), CM-BSO (+), or differentiation medium with NGF (50 ng/mL) for 1 h. Proteins extracted from each cell culture were resolved by SDS-PAGE, transferred to a membrane, and probed with anti-phosphorylated Erk1/2 (phospho Erk1/2), anti-Erk1/2, anti-phosphorylated p38 (phospho p38), anti-p38, anti-phosphorylated Smad1/5/8 (phospho Smad1/5/8), anti-phosphorylated Akt (phospho Ark) and anti-Akt. Actin was analyzed as an internal control. Numbers below blots indicate relative band intensities as determined by the ImageJ software.

signaling pathway in PC12 cells (Figure 2). Akt was 2-fold activated in both CM-BSO (−) and CM-BSO (+) treated PC12 cells, but no significant difference between the 2 groups was observed.

FGF2 and BMP2 are upregulated through p38 MAPK signaling in hADMPCs exposed to oxidative stress

We next examined which growth factors or cytokines from BSO-treated hADMPCs were involved in stimulation of neurite outgrowth. We found that both mRNA (Figure 3A and B) and protein (Figure 3C and D) levels for BMP2 and FGF2 were markedly increased in hADMPCs treated with BSO. To determine if this upregulation was caused by ROS, all cells were exposed to the antioxidant *N*-acetylcysteine (NAC). As we expected, addition of NAC to BSO-treated hADMPCs reduced the expression levels of BMP2 and FGF2 to control levels (Figure 3E and F). As BMP2 together with FGF2 has

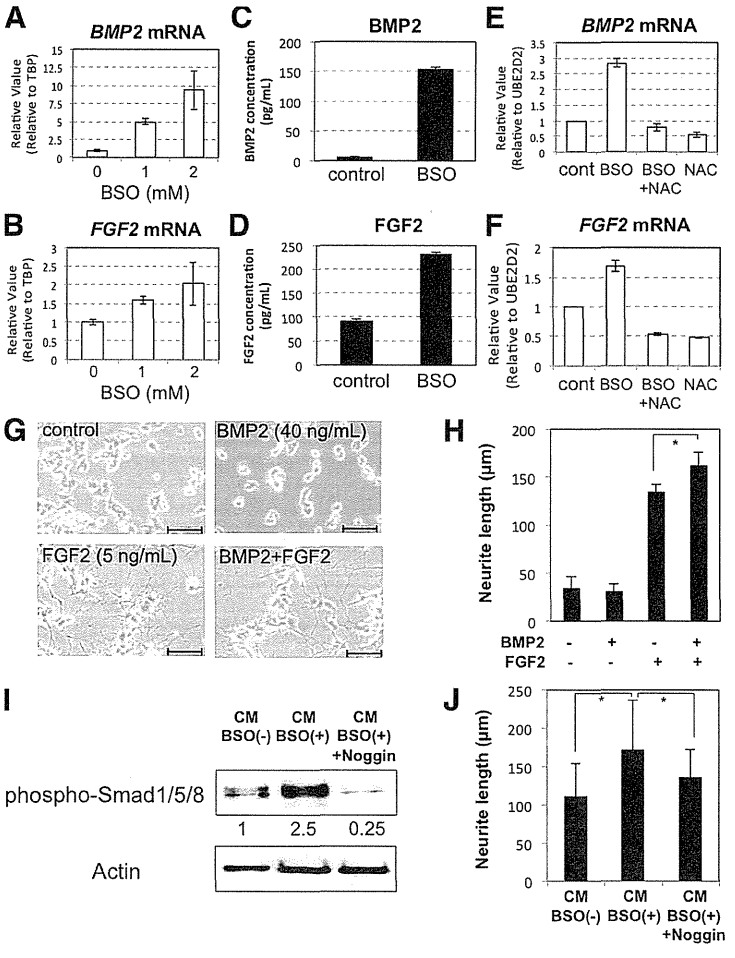

Figure 3 Transcription and secretion of BMP2 and FGF2 were increased in hADMPCs exposed to oxidative stress. (A, B) Upregulation of *BMP2* (**A**) and *FGF2* (**B**) mRNA in hADMPCs by BSO in a dose-dependent manner. **(C, D)** Secretion of BMP2 (**C**) and FGF2 (**D**) from hADMPCs in medium alone (cont) or with addition of 1 mM BSO (BSO) was analyzed by ELISA. **(E, F)** NAC treatment repressed the expression levels of *BMP2* and *FGF2* upregulated by BSO to the control levels. Expression of *BMP2* (E) and *FGF2* (F) mRNA was analyzed by q-PCR. cDNA was generated from total RNA extracted from hADMPCs (cont), hADMPCs treated with 1 mM BSO (BSO), 1 mM BSO + 5 mM NAC (BSO + NAC), and 5 mM NAC (NAC). The most reliable internal control gene was determined using the geNorm Software. **(G, H)** PC12 cells were cultured in differentiation medium alone (control), or differentiation medium supplemented with BMP2 (40 ng/mL), FGF2 (5 ng/mL), or both BMP2 and FGF2 (BMP2 + FGF2) for 2 days. (**G**) Representative images of neurite outgrowth in PC12 cells. Scale bars, 200 μm. (**H**) One hundred individual neurites were measured in each sample using Dynamic Cell Count Analyzer BZ-H1C (Keyence) and average neurite length was calculated. *, $P < 0.05$ (Student's t test). **(I, J)** PC12 cells were cultured in CM-BSO (−), CM-BSO (+), or CM-BSO (+) added with recombinant murine Noggin (200 ng/mL). **(I)** Western blot analysis of PC12 cells 1 h after CM treatment. Proteins extracted from each sample were resolved by SDS-PAGE, transferred to a membrane, and probed with anti-phosphorylated Smad1/5/8 (phospho-Smad1/5/8) and anti-Actin. Numbers below blots indicate relative band intensities as determined by the ImageJ software. (**J**) Two days after CM treatment, 100 individual neurites in PC12 cells were measured in each sample using Dynamic Cell Count Analyzer BZ-H1C (Keyence) and average neurite length was calculated. *, $P < 0.05$ (Student's t test).

previously been shown to induce neurite outgrowth in PC12 cells [26,27], we examined the effect of BMP2 and FGF2 on neurite outgrowth. We confirmed that PC12 cells did not differentiate effectively by BMP2 treatment alone, but BMP2 significantly augmented FGF2-induced neurite outgrowth in PC12 cells (Figure 3G and H), as previously reported. Moreover, in order to confirm the effect of BMP2 on neurite outgrowth in PC12 cells, 200 ng/mL of Noggin, an antagonist of BMP signaling, was added to CM-BSO(+). Addition of Noggin significantly suppressed the CM-BSO (+)-evoked phosphorylation of Smad1/5/8 (Figure 3I) and shortened the length of neurite outgrowth in PC12 cells (Figure 3J).

To address the question of which intracellular signaling pathways are affected by oxidative stress in hADMPCs, we focused on MAPK signaling since previous studies had suggested that accumulation of ROS in cells led to the activation of Erk1/2, p38, and JNK MAPK [28,29]. Western blotting revealed that BSO treatment markedly activated the p38 MAPK pathway; SB203580 could inhibit the activation, and U0126 treatment stimulated the activation (Figure 4A). ERK1/2 MAPK was significantly phosphorylated by BSO treatment, and ERK1/2 activation was reduced to the control level by treatment with U0126 (Figure 4B). In contrast, JNK activation was not observed in BSO-treated hADMPCs (Figure 4B). Therefore, we further investigated the relationship between increases in BMP2 and FGF2 expression and activation of the p38 and ERK1/2 MAPK signaling pathways by oxidative stress. Treatment

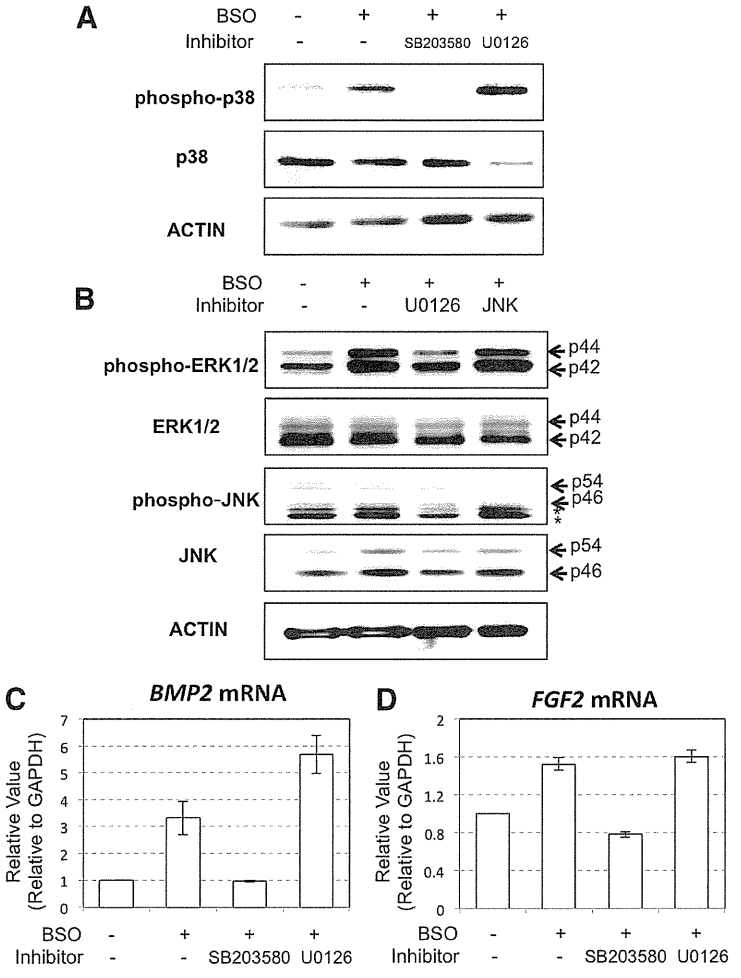

Figure 4 BMP2 and FGF2 were upregulated through activation of p38 MAPK. Inhibiton of p38 MAPK resulted in the supression of *BMP2* and *FGF2* transcripts upregulated by BSO treatment in hADMPCs. hADMPCs were pre-treated with 10 μM of SB203580, 10 μM of U0126 or 10 μM of JNK inhibitor II for 2 h followed by 1 mM BSO treatment for 16 h. The medium was replaced with fresh culture medium and the cells were cultured for another 2 days. **(A)** Western blot analysis of p38 MAPK activation in hADMPCs. **(B)** Western blot analysis of ERK1/2 MAPK, JNK SAPK activation in hADMPCs. **(C, D)** Transcription levels of *BMP2* (**C**) and *FGF2* (**D**) were analyzed by q-PCR. The most reliable internal control gene was determined using the geNorm Software.